Master Regenerative Medicine and Technology
Research report

The Effect of Endocrine Disrupting Chemicals Diethylstilbestrol and Ketoconazole on Bovine Oviduct Epithelial Cells Cultured in an Air-Liquid Interface Model and the use of this Model for Embryo Co-Culture

By

Jonna Simone van den Berg
5885523

October 2021- September 2022

Supervisors
Nadia Asimaki and Dr. Bart Gadella

Second examiner
Prof. Dr. Tom Stout

Department of Population Health Sciences, Farm Animal Health.
Faculty of Veterinary Medicine, Utrecht University, Utrecht, the Netherlands

Abstract

The worldwide problem of increasing frequency of female reproductive disorders is considered to be partially related to the rise in endocrine disrupting chemical (EDC) production and exposure. EDCs can interfere with normal hormonal action and regulation, and the effect of the two well described EDCs diethylstilbestrol (DES; a synthetic estrogen agonist) and ketoconazole (KTZ; a steroidogenic enzyme inhibitor) are examined on bovine oviduct epithelial cells (BOECs). In this thesis a 23-day BOEC monolayer culture in Transwell® inserts was established using the air-liquid interface (ALI) method to maintain the differentiated BOEC phenotype. BOEC-ALI cultures showed confluent monolayers with low percentage BOECs presenting secondary cilia at their apical membrane. In this culture system four-day exposure to DES or KTZ resulted in lowered lateral position of cell-cell adherence in a subpopulation of the BOECs, while BOEC viability and monolayer confluency was maintained. Furthermore, the use of the BOEC-ALI model for embryo co-culture did not result in the production blastocysts and cleavage rates were not as successful compared to conventional *in vitro* embryo production (IVP). Overall, a bovine oviduct model was established and proved functional as toxicological model. In order to apply this model to conduct embryo co-culture experiments and for the use as an indirect exposure toxicological model, the BOEC-ALI model needs to be further optimized.

Layman's summary

There is an increase in environmental presence of chemicals which are known to disrupt the hormone system of females. This is linked to the rise in female reproductive system disorders. When women are exposed to these chemicals before, or during, pregnancy there may be an effect on the embryo. Two classic chemicals known to affect the female reproductive system are diethylstilbestrol (DES) and ketoconazole (KTZ). However, little is known about their effect on the oviduct, the tube connecting the ovaries to the uterus. The oviduct is the place where an oocyte is fertilized by a sperm cell and further develops into an embryo. It is the first place of contact between mother and embryo and therefore of great importance for the earliest life stages. A key cell component of the oviduct are the epithelial cells (OECs) lining the oviduct cavity. Here, we culture these OECs which were obtained from cows, so that they form a single layer with tight cell-to-cell contact. When the OECs are cultured like this, they are called a monolayer. The OEC monolayers grow attached to a specialized plastic with very small pores to allow small molecules to pass. This specialized plastic barrier hangs in another plastic container, creating two compartments: above and under the plastic barrier. The compartment under the plastic barrier will be filled with culture medium, while the upper compartment containing the monolayer will be empty (filled with air). This is called an air-liquid interface (ALI) system, and this compartmentalization allows the OECs to maintain the same shape as in the oviduct in the body.

Here, we exposed the OECs from under the plastic barrier to DES and KTZ. We found that DES and KTZ exposure caused the OECs to lose the connections between them at their sides. However, this was not over the entire side, but starting from the middle to the top of the cells. Interestingly, exposure to DES or KTZ did not alter the monolayer, since the liquid from the bottom compartment did not transfer to the air-filled upper compartment. Thus, exposure to DES and KTZ altered cell-cell attachment, but the ALI system and the monolayer was maintained.

Since early embryo development takes place in the oviduct, we cultured fertilized oocytes in the upper compartment of the OEC-ALI system, on top of the OEC monolayers. This embryo culture was performed to establish an indirect exposure model, where DES and KTZ are potentially added to the lower compartment and separated from the embryo by the OEC monolayer. Unfortunately, we were only able to produce very early-stage embryos that did not progress through development, which is normally possible with other standardized protocols for embryo production. Therefore, indirect exposure was not performed.

Overall, this OEC-ALI model can be used to test the effect of toxic chemicals on oviduct epithelial cells. Here, we have shown that DES and KTZ induce loss of cell-cell attachment at the sides, while the monolayer was maintained. Furthermore, embryo culture in the OEC-ALI system was not successful. Since the oviduct environment is important during early embryo development, the OEC-ALI system should be further optimized to allow embryo culture.

Index

Introduction

For a long time, the oviduct was considered a passive channel for gametes and embryos, and its function for the female reproductive system was overlooked (Pérez-Cerezales et al., 2018). Yet, the oviduct is the first embryo-maternal contact zone and plays a pivotal role in gamete transport, sperm selection, fertilization, early embryo development, as well as genetic and epigenetic reprogramming (Almiñana et al., 2017; Ferraz et al., 2017; González-Brusi et al., 2020; Pérez-Cerezales et al., 2018). After ovulation, the released oocyte enters the oviduct where it will be fertilized by one sperm cell. After this fertilization, the early bovine embryo resides in the oviduct for approximately 3-4 days while it undergoes the first embryonic cleavages and from the 8-cell stage the embryonic genome becomes activated (Maillo et al., 2015; Rizos et al., 2017). The oviduct, which connects an ovary to the uterus, is composed of three regions: the infundibulum, the ampulla, and the isthmus. Pseudostratified columnar epithelium lines the lumen of the oviduct, and consists of ciliated epithelial cells that actively transport oocytes, sperm, and early embryos, and secretory epithelial cells which produce an optimized environment (Leese et al., 2001; Rottmayer et al., 2006). Previous studies have shown that the estrous cycle affects the morphology and function of oviduct epithelial cells (OECs). The key hormones of the cycle are progesterone (P4) and 17β-estradiol (E2), and circulate in the systemic bloodstream to reach OECs from the basolateral side (Chen et al., 2013a; Lopera Vasquez et al., 2022; Yániz et al., 2000). Around ovulation, during the follicular phase when E2 levels are high, the oviduct epithelium is predominated by ciliated OECs especially in the infundibulum and ampulla. Fewer changes are observed in the isthmus. In contrast, during the luteal phase, when P4 levels are high, there is an extensive distribution of secretory OECs (Abe & Oikawa, 1993; Yániz et al., 2000). Consistent with the morphological changes of the OECs, cycle-dependent changes in gene expression have been observed. During the luteal phase, genes involved in proliferation are upregulated. In contrast to this, genes involved in protein secretion are upregulated during the follicular phase. An example of this is increased secretion of oviductal glycoprotein 1 (OVGP1) which is the most abundant glycoprotein in the bovine oviductal fluid (Lopera Vasquez et al., 2022; Rottmayer et al., 2006; Zhao et al., 2022).

Due to human activities the environment is polluted with many toxic molecules and part of them typically have hormone like activities (either as agonist or antagonist) and these can be classified as endocrine disrupting chemicals (EDCs). EDCs are defined as exogenous substances or mixtures that alter function(s) of the endocrine system and consequently cause adverse health effects in an intact organism, or its progeny, or (sub) population (International Programme on Chemical Safety, 2002). The worldwide problem of the increasing frequency of (female) reproductive disorders is considered to be related to the rise in EDC production and exposure (Delbes et al., 2022; Ding et al., 2020; Ma et al., 2019). Currently, around 60 chemicals have been classified as EDC which are found in agriculture, consumer products, pharmaceutical drugs, cosmetics, and food packaging. Furthermore, it is suggested that exposure to EDCs can also be a result of contaminated water, air, or food (Brevini et al., 2005; Delbes et al., 2022). This thesis deals with the effects of two well described EDCs (diethylstilbestrol; DES and ketoconazole; KTZ) on OECs in the bovine species, which has not been studied in detail. DES, a synthetic estrogen receptor agonist, is a transplacental chemical that was prescribed for almost 30 years to pregnant women for the prevention of miscarriages. When adverse health effects in the *in utero* exposed daughters, such as clear-cell adenocarcinoma at young age and infertility occurred, the use of DES as pharmaceutical drug was terminated in 1972 (Adedeji et al., 2012; Dodds et al., 1938; Giusti et al., 1995; Herbst et al., 1971). The discovery of adverse health effects caused by DES led to the start of studies focusing on the mechanism of DES and its effect on the reproductive system. The properties of DES are similar to physiological estrogens and its effect is mediated through both nuclear estrogen receptor (ER) activation, and plasma membrane receptor activation (Adam et al., 2020; Bolger et al., 1998; Nadal et al., 2000). The consequences of DES exposure are broad and reach most tissues of the female reproductive system. However, little is reported about the effect on the oviduct. Another example of a classic EDC is KTZ, which is worldwide used to treat

mammalian fungal infections and fungicides in agriculture (Kjærstad et al., 2010). The antifungal property of KTZ relies on the inhibition of a specific cytochrome P450 enzyme, CYP51, which is essential for the production of sterols for the fungal membrane (Zarn et al., 2003). However, KTZ is not specific to fungal CYP enzymes but also interacts with the mammalian CYP enzyme system which is involved in the steroidogenic pathway (Loose et al., 1983; Sonino, 1987) and thus KTZ can be considered as an EDC. The formerly used topical and systemic antifungal pharmaceutical interfered with both androgen and estrogen synthesis resulting in decreased formation of estradiol and testosterone, and an increase of progesterone, indicating that KTZ interferes with the steroidogenic pathway (Baravalle et al., 2018; Kjærstad et al., 2010; Loose et al., 1983; Munkboel et al., 2019a; Sonino, 1987). Previous *in vivo* animal studies showed teratogenic and embryotoxic effects of systemic KTZ (King et al., 1998), as well as *in vitro* studies showed that high concentrations of KTZ caused degeneration of follicles and oocytes (Tsafriri et al., 1998). As mentioned before, little is reported about the effect of both DES and KTZ exposure on the bovine oviduct. Previous studies of *in utero* DES exposure in rats, mice, and chickens, showed oviductal abnormalities including inflammatory lesions and hypercellularity of oviductal stromal cells (Alwis et al., 2011; Newbold et al., 1983; Rothschild et al., 1987; Seo et al., 2009). Furthermore, a study showed the competence of fluconazole, another potent EDC from the azole antifungal family, to penetrate into female reproductive tract tissues, including the oviduct, but the local effect on the tissue is not reported (Mikamo et al., 1999; Munkboel et al., 2019b).

Despite the concern regarding little knowledge about the effects of DES and KTZ on the oviduct, there are considerable downsides to current oviduct epithelial cell culture methods. Oviduct function *in vitro* has predominantly been studied using bidimensional cultures, where OECs are cultured as monolayers or using oviduct explants in tissue culture flasks or petri dishes. When OECs are cultured in these bidimensional cultures, they rapidly dedifferentiate into flattened cells and lose their morphologic properties such as cell height, columnar shape, and cell polarity, as well as the functional properties of secretion activity and ciliation (Bissell, 1981; Ferraz et al., 2017; Gualtieri et al., 2012; Inman & Bissell, 2010; Reischl et al., 1999; Ulbrich et al., 2010). Given the importance of these properties for oviductal function, *in vitro* culture conditions should be established to preserve this. In contrast to bidimensional cultured OECs, the three-dimensional air-liquid interface (ALI) culture can support tissue specific characteristics, cell polarity and morphology of the OECs. The ALI culture forces confluent OEC monolayers to differentiate and has been established for monkey, equine, mice, porcine and bovine oviduct epithelial cell isolates (Chen et al., 2013b, 2017; Leemans et al., 2022; Rajagopal et al., 2006). The ALI culture uses compartmentalization, creating an apical and basolateral compartment, to stimulate cell polarity and differentiation. This compartmentalization provides the opportunity for embryo co-culture at the apical compartment, while the OECs are nourished from the basolateral compartment through the membrane of the Transwell® system. As previously mentioned, the oviduct is the specific environment where besides fertilization also the first days of embryonic development will take place. Multiple studies have shown that co-culture with BOECs and early embryos will stimulate early embryonic development (Abe & Hoshi, 1997; Galli et al., 2003; Gandolfi & Moor, 1987; Thibodeaux & Godke, 1992). There is increasing interest in the advancing of embryo co-cultures with more sophisticated and three-dimensional culture systems. Embryo co-culture in a Transwell® OEC-ALI system has already been described in literature using porcine, mice and bovine material (Chen et al., 2017; Jordaens et al., 2020). However, the resulting blastocyst yields were not comparable to conventional *in vitro* embryo production (IVP), and blastocyst quality was not examined (Chen et al., 2017; Jordaens et al., 2020). In addition to the potential beneficial effect on embryo co-culture, the OEC-ALI co-culture could be used as model for indirect toxicological exposure of embryos. The embryo would be indirectly exposed to toxins present in the basolateral compartment and separated by the confluent OEC monolayer. Documented effects of EDCs on the developing embryo are mostly from direct exposure, however, this does not mimic physiological exposure via the systemic circulation where for instance EDCs have to pass through the OECs to come in contact with the embryo (Amir et al., 2018; Gardiner et al., 1988; Santos et

al., 2014; Walker et al., 2000). Indirect exposure using an OEC-ALI (co-culture) system would give a better understanding of the effects of EDCs on the developing embryo, and the effects on OECs.

In this thesis, I have aimed to create a differentiated and confluent BOEC-ALI culture, which will be used to gain better understanding on the effects of DES and KTZ on BOECs. Its use for bovine embryo co-culture was tested. The results will be discussed with special emphasis on the effects of KTZ and DES on differentiation parameters such as cell viability, morphology, ciliation and monolayer confluency.

Materials and methods

Media solutions

Bovine oviduct epithelial cell air-liquid interface culture

DMEM/F-12: Dulbecco's Modified Eagle Medium F-12 Nutrient Mixture (DMEM/F-12; #31331-028 Gibco, Grand Island, NY, United States) supplemented with 10% fetal bovine serum (FBS; #F7524 Sigma-Aldrich, St. Louis, MO, United States), 5µg/mL insulin (#I0516 Sigma-Aldrich, St. Louis, MO, United States), 5µg/mL apo-transferrin (#T1428 Sigma-Aldrich, St. Louis, MO, United States), 10 ng/mL Epidermal Growth Factor (EGF; #4127 Sigma-Aldrich, St. Louis, MO, United States), 100 U/mL penicillin and 100 µg/mL streptomycin (#15140 Gibco, Grand Island, NY, United States), 50 µg/mL Gentamycin (#15750 Gibco, Grand Island, NY, United States), and 1µg/mL Amphotericin B (#A2942 Sigma-Aldrich, St. Louis, MO, United States).

In vitro embryo production (IVP)

Maturation media: M199 with Earle's salts and glutamine (#31100-027 Gibco, Grand Island, NY, United States) was buffered with 2.2% (g/L) $NaHCO_3$ with an osmolarity of 280-290 mOsm and sterilized through a 0.22 µm filter. This buffered media was supplemented with 100 U/mL penicillin and 100 µg/mL streptomycin (#15140 Gibco, Grand Island, NY, United States), 0.05 IU/ml recombinant hFSH (Organon), 0.1 µM cysteamine (#M9768 Sigma-Aldrich, St. Louis, MO, United States), and 10 ng/ml EGF (#E4127 Sigma-Aldrich, St. Louis, MO, United States).

Rinsing medium R: MilliQ supplemented with 0.11M NaCl (#1.06404.1000 Merck, Kenilworth, NJ, United States), 3.15 mM KCl (#4936 Merck, Kenilworth, NJ, United States), 2.00 mM $NaHCO_3$ (#S4019 Sigma-Aldrich, St. Louis, MO, United States), 0.33 mM Na_2HPO_4 (#6559 Merck, Kenilworth, NJ, United States), 0.13 % (v/v) sodium lactate (a 60% syrup solution; #L7900 Sigma-Aldrich, St. Louis, MO, United States), 9.99 mM HEPES (#H6147-100g Sigma-Aldrich, St. Louis, MO, United States), 0.2% (v/v) phenol red (#P0290 Sigma-Aldrich, St. Louis, MO, United States), 2.65 mM $CaCl_2.2H_2O$ (#2382 Merck, Kenilworth, NJ, United States), 0.49 mM $MgCl_2.6H_2O$ (#5833 Merck, Kenilworth, NJ, United States), 1.0 mM sodium pyruvate (#P2256 Sigma-Aldrich, St. Louis, MO, United States), 100 U/mL penicillin-streptomycin (#15140 Gibco, Grand Island, NY, United States), 0.6% (w/v) bovine serum albumin fraction V (#81003 MP Biomedicals, Santa Ana, CA, United States). The pH was measured and adjusted to 7.3 ± 0.05 and osmolarity was set to 280 ± 2 mOsm. The rinsed medium was filter sterilized (0.22 µm) and stored at -20 °C in aliquots.

Medium D 10X (D10X) was necessary for the dilution of Percoll®. LAL reagent water (#W50-500 Cambrex, East Rutherford, NJ, United States) supplemented with 0.9 M NaCl (#1.06404.1000 Merck, Kenilworth, NJ, United States), 30.85 mM KCl (#4936 Merck, Kenilworth, NJ, United States), 3.31 mM Na_2HPO_4 (#6559 Merck, Kenilworth, NJ, United States), 4.29 % (v/v) sodium lactate (a 60% syrup solution; #L7900 Sigma-Aldrich, St. Louis, MO, United States), 0.1 M HEPES (#H6147-100g Sigma-Aldrich, St. Louis, MO, United States), 15.25 mM $MgCl_2.6H_2O$ (#5833 Merck, Kenilworth, NJ, United States), 2 % (v/v) phenol red (#P0290 Sigma-Aldrich, St. Louis, MO, United States). The pH was measured and adjusted to 7.35 ± 0.05 and osmolarity was set to 280 ± 2 mOsm. D10X was filter sterilized (0.22 µm) and stored at 4 °C.
Medium D 1x (D1X) was used for Percoll® dilution and for sperm medium. D1X was produced by diluting D10X 10 times with LAL reagent water supplemented with 2% (v/v) phenol red (#P0290 Sigma-Aldrich, St. Louis, MO, United States).

Sperm medium: D1X supplemented with 1 mM sodium pyruvate (#P2256 Sigma-Aldrich, St. Louis, MO, United States), 100 U/mL penicillin-streptomycin (#15140 Gibco, Grand Island, NY, United States), and 0.6% (w/v) bovine serum albumin fraction V (#81003 MP Biomedicals, Santa Ana, CA, United States). Sperm medium was filter sterilized and stored at -20 °C in aliquots.

Percoll® solutions*:* Percoll® (#GE 17-5445-02 GE Healthcare, Chicago, IL, United States) was diluted 1:9 with medium D10X to establish 90% Percoll® solution. Percoll® 45% solution was established by a 1:1 dilution of Percoll® 90% with medium D1X. All Percoll® solutions were stored at 4°C.

Fertilization medium E: LAL reagent water (#W50-500 Cambrex, East Rutherford, NJ, United States) supplemented with 0.11 M NaCl (#1.06404.1000 Merck, Kenilworth, NJ, United States), 3.09 mM KCl (#4936 Merck, Kenilworth, NJ, United States), 25.0 mM $NaHCO_3$ (#S4019 Sigma-Aldrich, St. Louis, MO, United States), 0.33 mM Na_2HPO_4 (#6559 Merck, Kenilworth, NJ, United States), 0.22 mM sodium pyruvate (#P2256 Sigma-Aldrich, St. Louis, MO, United States), 0.2% (v/v) phenol red (#P0290 Sigma-Aldrich, St. Louis, MO, United States), 2.65 mM $CaCl_2.2H_2O$ (#2382 Merck, Kenilworth, NJ, United States), 0.49 mM $MgCl_2.6H_2O$ (#5833 Merck, Kenilworth, NJ, United States), 100 U/mL penicillin-streptomycin (#15140 Gibco, Grand Island, NY, United States), 0.6% (w/v) BSA fatty acid free (#A6003 Sigma-Aldrich, St. Louis, MO, United States). The pH was measured and adjusted to 7.3 ± 0.05 and osmolarity was set to 280 ± 2 mOsm. Fertilization medium E was filter sterilized (0.22 µm) and stored at -20 °C in aliquots.

Penicillamine-hypotaurine-epinephrine (PHE) solution: 0.9% NaCl supplemented with 0.5 mM penicillamine (#4875 Sigma-Aldrich, St. Louis, MO, United States), 0.5 mM hypotaurine (#1384 Sigma-Aldrich, St. Louis, MO, United States), and 25 µM epinephrine (#E1635 Sigma-Aldrich, St. Louis, MO, United States). Penicillamine and hypotaurine were dissolved in 0.9% NaCl, whereas epinephrine was dissolved in sterile solution A. PHE solution was stored at -20 °C.
Solution A: LAL reagent water (#W50-500 Cambrex, East Rutherford, NJ, United States) supplemented with 2.52 % (v/v) sodium lactate (a 60% syrup solution; #L7900 Sigma-Aldrich, St. Louis, MO, United States), and 52.60 mM sodium metabisulfite (#S900 Sigma-Aldrich, St. Louis, MO, United States). pH was set at 4, and solution A was stored at -20 °C.

Synthetic oviductal fluid (SOF) media*:* SOF media was composed of 1:4 ratio of SOF A and SOF B. *SOF A*: LAL reagents water (#W50-500 Cambrex, East Rutherford, NJ, United States) supplemented with 0.13 M NaCl (#S5886 Sigma-Aldrich, St. Louis, MO, United States), 8.95 mM KCl (#4936 Merck, Kenilworth, NJ, United States), 1.49 mM KH_2PO_4 (#P5655 Sigma-Aldrich, St. Louis, MO, United States), 0.075 % (v/v) sodium lactate (a 60% syrup solution; #L7900 Sigma-Aldrich, St. Louis, MO, United States), 0.92 mM MgSO4.7H2O (#105886500 Merck, Kenilworth, NJ, United States), 31.24 mM $NaHCO_3$ (#S4019 Sigma-Aldrich, St. Louis, MO, United States), 2.22 mM $CaCl_2.2H_2O$ (#2382 Merck, Kenilworth, NJ, United States), 0.0625 % (v/v) phenol red (#P0290 Sigma-Aldrich, St. Louis, MO, United States), 1.25% (v/v) MEM NEAA (#M7145 Sigma-Aldrich, St. Louis, MO, United States), 2.5% (v/v) BME AA (#B6766 Sigma-Aldrich, St. Louis, MO, United States). The pH was adjusted to 7.3 ± 0.05 and osmolarity was set to 300 ± 2 mOsm. SOF A was filter sterilized (0.22 µm) and stored at 4°C. *SOF B*: LAL reagents water (#W50-500 Cambrex, East Rutherford, NJ, United States) supplemented with 100 U/mL penicillin-streptomycin (#15140 Gibco, Grand Island, NY, United States), 1.64 mM sodium pyruvate (#P2256 Sigma-Aldrich, St. Louis, MO, United States), 10.26 mM L-glutamine (#G8540 Sigma-Aldrich, St. Louis, MO, United States), 2% BSA (#81-001-4 Merck, Kenilworth, NJ, United States). The pH was adjusted to 7.3 ± 0.05. SOF B was filter sterilized (0.22 µm) and stored at 4°C.

Methods

Experimental design

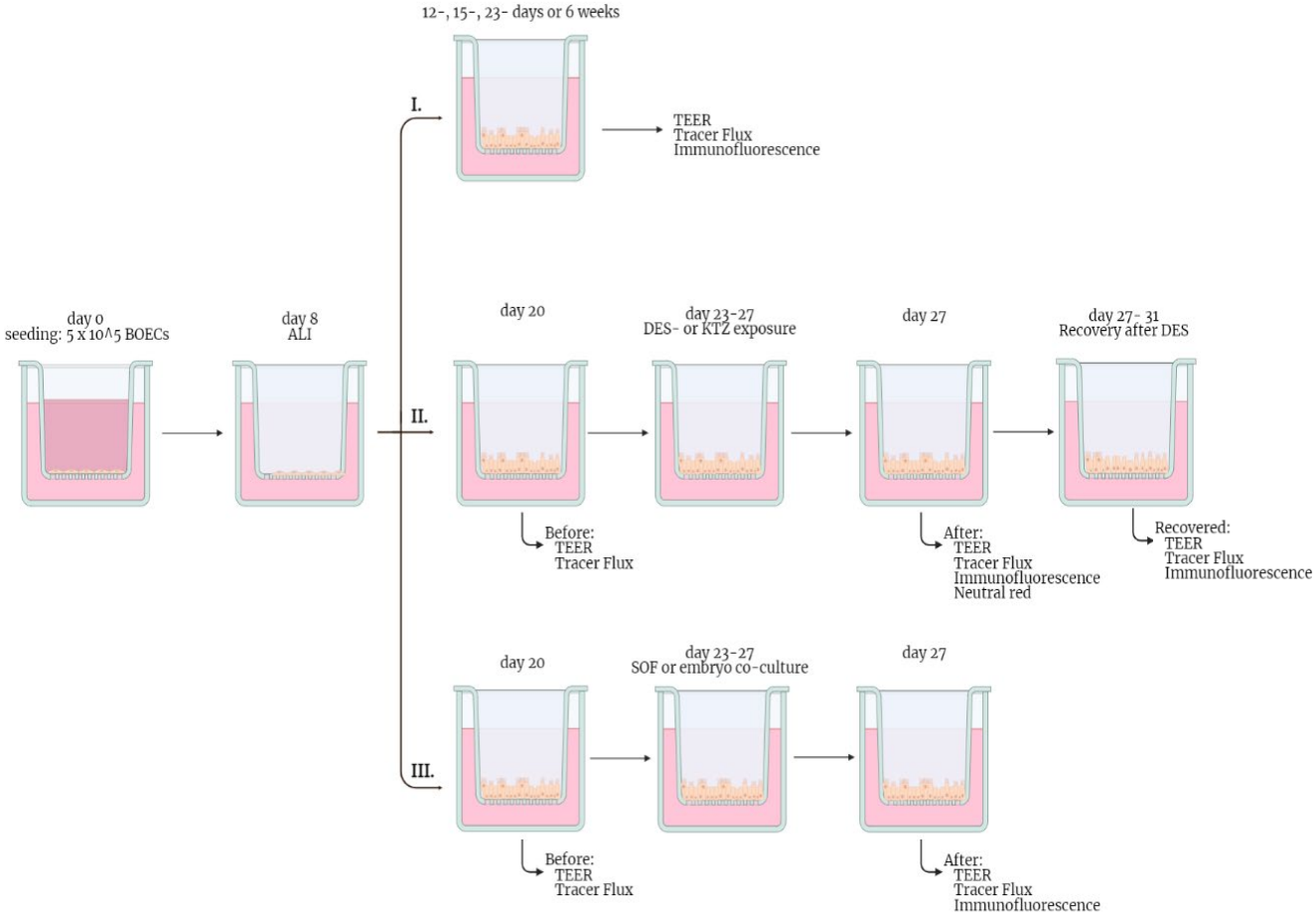

Scheme 1: Experimental design to establish confluent monolayers of bovine oviduct epithelial cells (BOECs) on microporous membrane in Transwell® inserts. Mechanically isolated BOECs were cultured from day 0-8 in liquid-liquid interface, and at day 8 air-liquid interface (ALI) was introduced. I) establishment of differentiated BOEC monolayer. BOECs monolayers were cultured for various durations. Confluency was assessed with transepithelial electrical resistance (TEER) measurement and paracellular tracer flux assay. BOEC morphology and differentiation was analysed with immunofluorescence. II) Effect of diethylstilbestrol (DES) and ketoconazole (KTZ) exposure on the BOEC monolayer. Three days before exposure, day 20, confluency was assessed with TEER and tracer flux measurement. Monolayers were exposed to DES, KTZ or vehicle from day 23-27. After exposure, day 27, confluency was assessed, as well as BOEC morphology and differentiation (immunofluorescence). Additionally, BOEC viability after exposure was assessed using the neutral red assay. Only DES treated monolayers were cultured from day 27-31 under normal conditions, to observe whether they recover after DES exposure. III) Embryo co-culture in BOEC-ALI system. Same measurements at day 20 and day 27 were performed as in section II, except viability of BOECs was not determined. Overview of number of replicates and total monolayers used per experiment is depicted in Supplemental table 1.

Bovine oviduct epithelial cell (BOEC) air-liquid interface (ALI) culture

Bovine uteri with oviducts still attached were slaughter-house by-products and collected from slaughterhouse Gosschalk (Epe, Netherlands). Uteri were collected and transported on ice. Per each ALI culture, material of four animals was pooled, unless stated otherwise. One oviduct per animal was isolated and dissected from surrounding tissue, i.e., broad ligaments, mesosalpinx, and fat tissue. Oviducts were rinsed once in ice cold phosphate buffered saline (PBS; Fresenius Kabi) supplemented with 50 µg/mL gentamycin (#15750 Gibco, Grand Island, NY, United States), 100 U/mL penicillin-streptomycin (#15750 Gibco, Grand Island, NY, United States), washed once quickly in 70% ethanol, and rinsed two times in PBS supplemented with antibiotics. BOECs were mechanically isolated by squeezing, using tweezers, the oviduct from the infundibulum to the isthmus. BOECs were collected in 4 mL preheated (38 °C) M199 (#22340 Gibco, Grand Island, NY, United States) supplemented with 50 µg/mL gentamycin (#15750 Gibco, Grand Island, NY, United States) and 100 U/mL penicillin-streptomycin (#15140 Gibco, Grand Island, NY, United States). Cells were resuspended using a 18g needle (Sterican #4665120 B Braun, Melsungen, Germany), transferred to a 15 mL tube, and centrifuged for 5 min, 100 x *g* at 25 °C. Supernatant was removed and the BOECs were resuspended with 2 mL preheated (38 °C) M199 supplemented with antibiotics, and centrifuged under the same conditions. Supernatant was disposed, and BOECs were resuspended in 2 mL preheated (38 °C) DMEM/F-12. The cell suspension was divided over four wells of a 6 wells plate (F-bottom, CELLSTAR® #657160 Greiner Bio-one, Germany), containing 4 mL preincubated DMEM/F-12, and BOECs were incubated at 37 °C under 5% CO_2 for at least 24 hours.

Due to mechanical isolation, fibroblasts may have been isolated alongside of BOECs. BOECs have very low cell attachment efficiency in absence of extracellular matrix proteins, while fibroblasts attach quickly to the culture well (Abe & Hoshi, 1997; Alberts et al., 2002). Therefore, after 24h of incubation only the cells in suspension (oviduct epithelial cell aggregates with minimal amount of fibroblasts) were carefully collected, transferred to a 15 mL tube, and centrifuged for 5 min, 100 x *g* at 25 °C. Supernatant was removed and BOECs were resuspended in 1 mL DMEM/F-12. $5x10^5$ BOECs were seeded in the apical compartment of Transwell® inserts (CLS3413, polycarbonate membrane, 6.5 mm diameter, 0.4 µm pore diameter, apical-basolateral compartment volume: 150-800 µL, Costar, Corning, United States), and cultured at 37 °C under 5% CO_2. From day 1 to day 8 BOECs were cultured in a Liquid-Liquid Interface (LLI) meaning 150 µl DMEM/F-12 in the apical compartment, and 800 µl DMEM/F-12 in the basolateral compartment. At day 8 of culture, air-liquid interface (ALI) was introduced by removing the media from the apical compartment, while basolateral media was maintained. Basolateral DMEM/F-12 was refreshed three times a week. ALI was maintained until day 23, unless stated otherwise.

Pooled vs. non-pooled

Monolayers used to select BOEC culture period were established from pooled material. Pooling material could possibly limit differentiation of BOECs (Chen & Schoen, 2021), causing diminished percentage of BOECs with secondary cilia. Non-pooled monolayers were established from three individual animals, whereas the pooled monolayers combined BOECs of all three animals.

Endocrine disrupting chemical (EDC) exposure

BOEC monolayers were exposed from the basolateral side to EDCs from day 23 until day 27 of culture, while maintaining ALI. DMEM/F-12 was supplemented with either diethylstilbestrol (DES; #D4628-1G Sigma-Aldrich, St. Louis, MO, United States) or ketoconazole (KTZ; #K1003 Sigma-Aldrich, St. Louis, MO, United States), both dissolved in 0.01% v/v Dimethyl Sulfoxide (DMSO; D2650-5X Sigma-Aldrich, St. Louis, MO, United States). Final concentrations of 10^{-9} M, 10^{-7} M, 10^{-5} M DES and 10^{-8} M, 10^{-7} M, 10^{-6} M KTZ were reached. DES and KTZ concentrations were determined beforehand by the FREIA project. All experiments included two control groups; DMEM/F-12 supplemented with 0.01% DMSO (vehicle), and a control of only DMEM/F-12.

DES recovery
Following DES (10^{-9} M, 10^{-7} M, 10^{-5} M) exposure (day 23-27), monolayers were cultured under normal conditions (DMEM/F-12) from day 27-31, establishing a recovery period of four days.

Synthetic oviductal fluid (SOF) incubation
To test whether SOF affects the BOECs, from day 23-27 50-, 100-, or 150 µl pre-gassed SOF (5% CO_2, 7% O_2, 38.5°C) was placed in the apical compartment of Transwell® inserts containing BOECs. Monolayers that remained in ALI state served as control.

Embryo co-culture
For embryo co-culture in the apical compartment of Transwell® inserts containing established BOEC monolayers, presumed zygotes were produced via *in vitro* maturation and *in vitro* fertilisation (elaborate protocol see material and methods; methods: *in vitro* embryo production (IVP)). Presumed zygotes were cultured from day 1-5 in the apical compartment of Transwell® inserts containing BOEC monolayer. Day 1-5 of *in vitro* embryo culture (IVC) is in parallel with day 23-27 of BOEC monolayer culture. Groups of presumed zygotes in different numbers (6,15,20) and SOF volumes (100 µl, 150 µl) were tested for optimum blastocyst development. Groups were based on co-culture experiments performed in lab history, where IVC in apical compartment of Transwell® inserts was successful in ratio of 6 presumed zygotes in 60 µl SOF.

Analysis
Three days before (day 20) and directly after (day 27) EDC exposure, apical SOF incubation, or IVC co-culture, confluency of the BOEC monolayer was assessed using transepithelial electrical resistance (TEER) measurement and paracellular tracer flux assay. In addition, BOEC morphology and differentiation were analysed using immunofluorescence.

Trans-epithelial electrical resistance

BOEC monolayer confluency was assessed by transepithelial electrical resistance (TEER) measurements, based the on protocols of Chen et al., 2015 and Leemans et al., 2022. Ag/AgCl electrodes (MERSSTX01 Millipore, Burlington, MA, United States) were sterilized for 15 min in 70% ethanol, airdried, and connected to a Volt-Ohm meter (Millicell® ERS-2 Millipore, Burlington, MA, United States). Until use, electrodes were placed in M199 supplemented with 50 µg/mL gentamycin (#15750 Gibco, Grand Island, NY, United States) and 100 U/mL penicillin-streptomycin (#15140 Gibco, Grand Island, NY, United States) at RT. The resistance of M199 supplemented with antibiotics at RT was measured. Temperature fluctuations is known to have a strong effect on TEER values (Blume et al., 2010). To reduce this effect, TEER was performed on a heating plate of 38°C, directly after replacement of DMEM-F12 with pre-heated antibiotic-supplemented M199. To measure the resistance (Ohm), electrodes were inserted in both the apical and basolateral compartment. After a few second of stabilization, the resistance values were recorded. In parallel, resistance of empty control inserts, without BOECs, was measured (expected to range between 150 and 210 Ohm). The resistance of all inserts was measured in duplicate and averaged. TEER values in Ω*cm^2 were calculated as following:

$$R_{sample}(\Omega) = R_{total} - R_{blank}$$

$$TEER_{sample}(\Omega\ cm^2) = R_{sample}(\Omega) * Area_{membrane}(cm^2)$$

R blank was the resistance measured of empty inserts combined with the resistance measured of M199 supplemented with antibiotics at RT. The area of the membrane was 0,33 cm^2.

Paracellular tracer flux assay

To substantiate TEER values, confluency was assessed with a paracellular tracer flux assay, using a cell-impermeable fluorescent tracer. Tracer flux was performed directly after the TEER by replacing apical media with 150 µl of 12 µg/mL natrium fluorescein disodium salt (0.4 kDa, #F6377 Sigma-Aldrich, St. Louis, MO, United States) diluted in M199 supplemented with 50 µg/mL gentamycin (#15750 Gibco, Grand Island, NY, United States) and 100 U/mL penicillin-streptomycin (#15140 Gibco, Grand Island, NY, United States). Basolateral compartment maintained plain M199 supplemented with antibiotics. After a 2 h incubation in the dark at 37 °C under 5% CO_2, basolateral and apical media were recovered and stored at 4 °C in the dark. An empty insert without BOECs served as control. Fluorescence intensity was measured using a BMG Clariostar fluorimeter (Ortenberg, Germany), excitation was set at 483 nm, and emission at 530 nm. Media acquired from the apical and basolateral compartment was measured in duplicate in a 96-wells plate (F-bottom, CELLSTAR® #657160 Greiner Bio-one, Germany). Percentage of the tracer transferred from the apical to the basolateral compartment was calculated as followed:

$$Tracer\ Flux\ \% = \frac{Fluorescence\ Intensity\ basolateral\ compartment}{Total\ Fluorescence\ Intensity}\ x100\%$$

Where total fluorescence Intensity was the fluorescence intensity of the basolateral compartment combined with the fluorescence intensity of the apical compartment of one sample.

Whenever tracer flux assay was performed at day 20 (before), apical and basolateral compartment were washed twice with pre-heated DMEM/F-12. Subsequently, inserts were incubated again after fresh DMEM/F-12 was added to the basolateral compartment, and the apical compartment remained empty, maintaining ALI.

Neutral Red Cytotoxicity assay

Lysosomal neutral red uptake was measured to detect BOEC viability after EDC exposure, using the neutral red cell cytotoxicity assay kit (#K447-1000 BioVision, Milpitas, CA, United States). NRU is based on the ability of viable cells to incorporate and retain the dye in the lysosomes, whereas a dead cell does not have this ability. Viability was assessed after exposure, day 27. Measurement was performed according to the manufacturer's instructions. The monolayer was briefly washed with 200µl washing solution, following 2 h incubation at 37 °C with 150 µl neutral red staining solution. Cells were washed again before a 20 min incubation at RT with 150 µl solubilization solution. Viable cells release neutral red after solubilization, 50 µl of the medium of each monolayer was transferred in duplicate to a 96-well culture plate (F-bottom, CELLSTAR® #657160 Greiner Bio-one, Germany). Absorbance was measured at 540 nm using SPECTROstar^{Nano} (BMG Labtech, Ortenberg, Germany) microplate reader. As control, NR assay was performed with omitting the neutral red dye, these monolayers, and were incubated with DMEM for 2h.

$$\%Viability = \frac{OD_{sample}}{OD_{blank}}\ x100\%$$

OD_{sample} was the OD of the sample after background correction, and OD_{blank} was OD of neutral red solution after background correction.

Immunofluorescence of BOEC morphology and ciliation

When ALI culture was completed, BOEC morphology and ciliation were assessed using confocal microscopy. BOEC monolayers were fixed in PBS diluted 4% paraformaldehyde (PFA) (Electron Microscopy Sciences) in basolateral- and apical compartment, for 15 min at RT. Monolayers were rinsed twice with PBS for 5 min, whereafter BOECs were permeabilized and non-specific binding was blocked using PBS containing 0.5% v/v Triton X-100 (X-100 Sigma-Aldrich, St. Louis, MO, United States) and 5% v/v normal goat serum (GenWay Biotech Inc., San Diego, CA, USA), for 30min at RT. After two 5 min wash steps with 0.5% PBST, the monolayers were incubated with anti-acetylated α-tubulin primary antibody in 0.5% PBST (1:100 dilution, #sc-23950 Santa Cruz Biotechnology, Santa Cruz, CA, United States) overnight at 4 °C. Subsequently, monolayers were washed three times with 0.5% PBST for 5 min, and incubated with the secondary goat-anti-mouse antibody conjugated to Alexa 488 diluted in 0.5% PBST (1:100 dilution, #A11029 Invitrogen, Landsmeer, The Netherlands) for 2 h at RT. Monolayers were washed three times with 0.5% PBST for 5 min, whereafter the monolayers were incubated with Hoechst 33342 (250 µg/ml, #B2261 Sigma-Aldrich, St. Louis, MO, United States) and phalloidin (1:100 dilution, #A12380 Invitrogen, Landsmeer, The Netherlands) diluted in 0.5% PBST, for 1 h at RT. Monolayers were washed twice in PBS for 5 min, after which the membranes were excised from the insert using a surgical 11 blade (#0203 Swann-Morton, Sheffield, United Kingdom). The excised membranes were mounted on glass slides (#6311533 Avantor, Radnor Township, PA, United States) and topped with 15 µl Vectashield diluted in PBS (1:3 dilution, #H-1000 Vector Laboratories, Burlingame, CA, United States), covered with a coverslip and sealed with nail polish. Samples were stored in the dark at 4 °C until imaging.

Imaging was performed using Nikon A1R confocal microscope (Nikon, Tokyo, Japan), using a 40x objective with a numerical aperture (NA) of 1.3 or a 60x objective with a NA of 1.45. The 60x objective was only used for imaging the monolayers of the 12-, 15-, 23-day and 6-week monolayers. All other monolayers were imaged with the 40x objective. Three separate channels were used for visualization of chromatin (Hoechst 33342; excitation 405 nm), primary and secondary cilia (acetylated α-tubulin; excitation 488 nm, with a ND32 488 filter), and F-actin (phalloidin; excitation 561 nm). For each monolayer, at 10 random locations Z-stack images from top-to-bottom, with a step-size of 1 µm, were acquired. Secondary cilia and phalloidin analysis were performed on the first 5 images.

Automated cell count was conducted using Nikon NIS elements Imaging Software (Laboratory Imaging, version 5.21.03). For the 405-laser channel (Hoechst), 488-laser channel (anti-acetylated α-tubulin), and 561-laser channel (Phalloidin), Denoise.ai software was applied, followed by maximum intensity projection of all frames. Subsequently, exclusively for the 405-laser channel bright spot detection was applied: typical diameter: 8.0 µm, contrast: 2.87, symmetry: all objects, intensity: 55-4095, grow: 150, output: circular area. Bright spots were reported as nuclei, and batch analysis provided number of nuclei of each image. 3 random images were manually counted and compared to automated count, with a <1% discrepancy in number of nuclei. Secondary cilia were manually counted in each image and divided by the number of nuclei generated by the automated cell count.

In vitro embryo production (IVP)

Collection of oocytes and in vitro maturation (IVM)

Bovine ovaries were slaughterhouse by-products and obtained from slaughterhouse Gosschalk (Epe, Netherlands), and transported immediately in a thermos flask. Ovaries were rinsed with water of 30°C, and collected in 0.9% NaCl (#211928001 B Braun, Melsungen, Germany) supplemented with 0.1% (v/v) penicillin-streptomycin (#15140 Gibco, Grand Island, NY, United States), and placed in a waterbath of 30°C until use. Cumulus oocyte complexes (COCs) were aspirated from follicles with a 2-8mm diameter, using a 18g needle (#40018 Vasuflo Dispomed, Gelnhausen, Germany) connected to a 50 mL tube, under vacuum with a low flow rate to minimise damage of COC integrity. Sediment was transferred to a petri dish with grid, and individual COCs were collected using a stereomicroscope. Selection of COCs was based on morphology; presence of a clear zona pellucida, healthy cumulus layer and a slightly darker ooplasm. COCs with a star-like appearance, denuded cumulus or dark ooplasm, were excluded. Selected COCs were collected in clear follicular fluid and washed twice in HEPES-buffered M199 media (#22340 Gibco, Grand Island, NY, United States), and once rinsed with pre-incubated maturation medium. 35-70 COCs were placed in 500 µl pre-incubated maturation medium in a 4-well plate and were placed in a 5% CO_2 incubation at 39°C for 22-24h.

In vitro fertilization (IVF)

For all IVF experiments sperm from the same bull was used, identification number NLDM000264706704, breed Meuse-Rhine-Yssel (MRY bull), purchased from CRV (Arnhem, Netherlands). Sperm was cryopreserved in liquid nitrogen, and after 22-24h of IVM, sperm was thawed for 1 min at 38°C, deposited on a 45%-90% Percoll® gradient, and centrifuged at 700 x *g*, 27°C for 30 min. Sperm mobility was checked under a light microscope. Simultaneously, COCs were rinsed twice in pre-warmed rinsing medium R, transferred to 430 µl pre-incubated fertilization medium E in a 4-well plate, and temporarily placed back in the incubator. Subsequently, the Percoll® supernatant was discarded, and the sperm pellet was resuspended in 50µl pre-warmed sperm medium. Sperm concentration was determined, fertilization medium containing washed COCs was supplemented with 20 µl 0.25 mg/ml heparin (#H3393 Sigma-Aldrich, St. Louis, MO, United States), 20 µl PHE solution, and 0.5 x 10^6/mL sperm. COCs and sperm cells were co-incubated for 18-22 h in a 5% CO_2 incubator at 39°C.

In vitro Embryo Culture (IVC)

After 18-22 h of fertilization presumed fertilized oocytes, or presumed zygotes, were denuded from the cumulus cells by vortexing for 3 min in pre-warmed rinsing medium R. The denuded presumed zygotes were washed twice in pre-warmed rinsing medium R, and transferred to 500 µl pre-incubated SOF medium (5% CO_2, 7% O_2, 38.5°C), and cultured in a 5% CO_2, 7% O_2 incubator at 38.5°C. At day 5 of IVC the cleavage rate was assessed by categorizing the embryos based on cell number: un-cleaved, ≤8-cell embryos, or >8-cells embryos. The un-cleaved cells were removed, and the cleaved embryos were transferred to 500µl fresh pre-incubated SOF medium. On day 7 and 8 of IVC blastocyst numbers were noted. Cleavage rate at day 5 was calculated by dividing all cleaved embryos (≤8 cells and 8 cells embryos) by total presumed zygotes. Blastocyst rate at day 7 and 8 was calculated by dividing the number of blastocysts by the total presumed zygotes initially incubated.

Embryo co-culture in the BOEC-ALI model

Presumed zygotes were co-cultured in the apical compartment of BOEC-ALI Transwell® inserts from IVC day 1-5. Following steps differ compared to conventional IVC protocol. 6-, 15- or 30 presumed zygotes were transferred to 100- or 150 µl pre-incubated SOF medium (5% CO_2, 7% O_2, 38.5°C) in the apical compartment of BOEC-ALI Transwell® inserts. At day 5 cleavage rate was determined, the un-cleaved cells were removed, and the cleaved embryos were transferred to 100 or 150 µl fresh pre-incubated SOF medium in a 96-wells plate (U-bottom, CELLSTAR® #650101 Greiner Bio-one, Germany) and cultured until day 8.

Statistical analysis

All experiments were performed with BOECs established from pooled biological material, unless stated otherwise. One-way ANOVA with Games-Howell post hoc test was used for all statistical comparisons for 12, 15, 23-day ALI culture, as well as for pooled vs. non pooled culture. Paired-sample student *t*-test was used for TEER, tracer flux, and percentage BOECs with secondary cilia comparison between two time points (e.g., day 20 vs. day 27) for one condition. Difference of these parameters between multiple conditions was analysed using one-way ANOVA. Before one-way ANOVA was performed, homogeneity of variances was tested using Levene's test ($P<0.05$). Equal variances were not assumed; therefore Games-Howell post hoc test was used for one-way ANOVA. Comparison of lateral cell-cell adherence position was based on categories and was analysed using non-parametric Kruskal-Wallis H test. The relationship between occurrence of lowered position of lateral cell-cell adherence and TEER- or tracer flux development were determined using Spearman correlation coefficient. All analysis were performed using IMB SPSS Statistics version 28.0.1.0 for windows (IMB Corp, Armonk, NY, United states).

Results

I. Establishment of a differentiated bovine oviduct epithelial cell monolayer

Duration of the air-liquid interface culture

First, the optimal duration of air-liquid interface (ALI) bovine oviduct epithelial cell (BOEC) culture was determined to optimise the establishment of a confluent monolayer of differentiated BOECs. BOEC monolayers were cultured for either 12, 15 or 23 days. A 6-week culture was also established, albeit from different biological material, and therefore unfit for direct statistical comparison to the other culture durations. BOEC monolayers reached confluency after 12 days of culture, as confirmed by high transepithelial electrical resistance (TEER) and low percentages of paracellular tracer flux. Prolonging culture, from 12 to 15 or 23 days, resulted in a non-statistically significant decrease in TEER values (1539±254 $\Omega*cm^2$, 1317±242 $\Omega*cm^2$, 1140±76 $\Omega*cm^2$, respectively; Figure 1A). TEER values of the 6-week culture were noticeably lower, 455±127 $\Omega*cm^2$, however they cannot be statistically compared (Figure 1B). The paracellular tracer flux assay further substantiated the confluency of all monolayers. Specifically, there was restricted passage of 0.4 kDa natrium fluorescein disodium salt from the apical compartment to the basolateral compartment. Total percentage of tracer transferred over the BOEC monolayer was <0.4% in all cultures (Figure 1C-D).

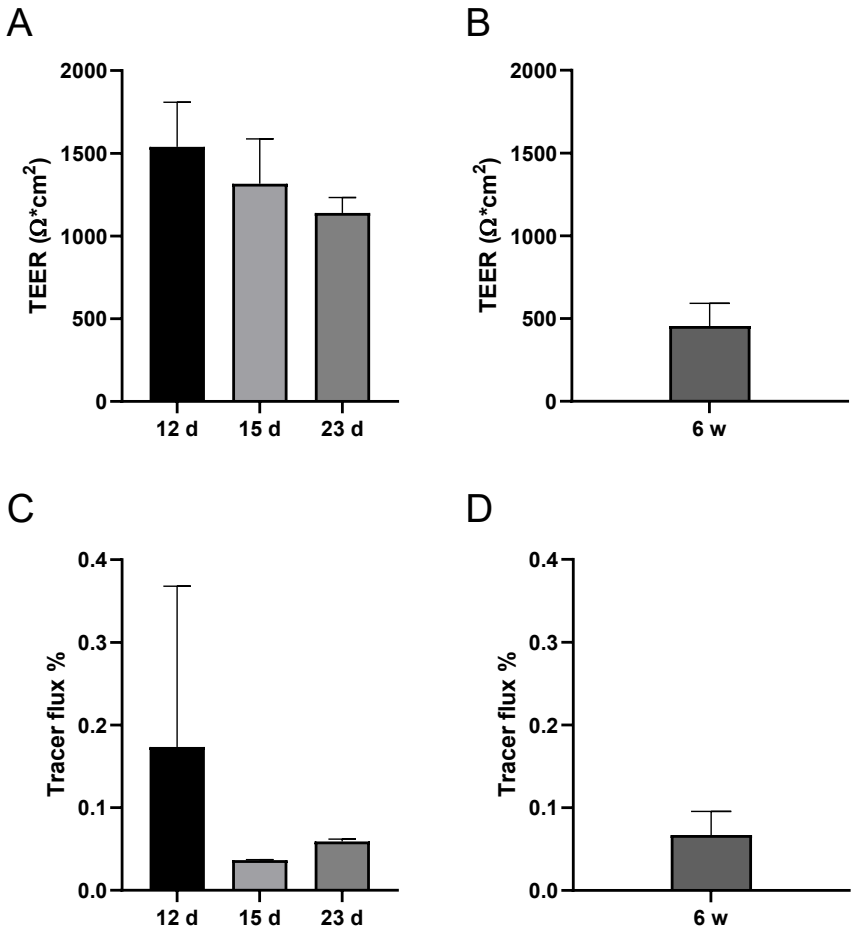

Figure 1: BOEC monolayers after 12-, 15-, 23 days or 6 weeks of culture in Transwell® inserts. Monolayers of shorter culture duration were established from the same biological material, and the 6-week monolayer from distinct biological material. Bars represent mean ± SD of one replicate. TEER measurement performed on BOEC monolayers cultured for 12, 15 or 23 days (A) and 6 weeks (B). Total percentage tracer flux detected in basolateral compartment was low (<0.4%) in BOEC monolayers cultured for 12, 15 or 23 days (C) and 6 weeks (D).

In vivo, oviducts are lined with a columnar pseudostratified epithelium with ciliated and non-ciliated cells (Kress & Morson, 2007). The morphology and differentiation of *in vitro* cultured BOEC monolayers were examined. BOEC monolayers of all cultures (12-, 15-, 23-days, 6-weeks) showed *in vivo*-like columnar pseudostratified morphology and organisation, comprising of a single cell layer with oval-shaped nuclei disposed at different levels. Additionally, BOECs showed tight lateral cell-cell adherence and cell-membrane attachment, observed with phalloidin (F-actin) labelling, further supporting confluency of all BOEC cultures. However, compared to the 23 days (Figure 2C) and 6 weeks (Figure 2D) BOEC cultures, BOECs cultured for 12 (Figure 2A) and 15 days (Figure 2B) showed more irregular morphology which presented as phalloidin (F-actin) staining in dots at the apical side of the cells. Another aspect of differentiated epithelial cells investigated was the development of cilia on the apical membrane of the BOECs (see Figure 3C for examples). BOECs with primary and secondary cilia were observed to localise in clusters, rather than evenly dispersed. A low percentage (≤5.6%) of secondary cilia was recorded for all BOEC monolayers, but a 23 day long culture resulted in statistical significantly more secondary cilia compared to the 12 and 15 day culture (2.29±2.21% vs. 0.16±0.41% and 0.43±1.1%, respectively; Figure 3A). Of all cells analysed from monolayers cultured for 6 weeks, 0.94±0.75% displayed secondary cilia (Figure 3B). In conclusion, BOEC monolayers reach confluency after 12 days of culture, and mimic aspects of barrier function of *in vivo* oviduct epithelium. However, BOECs cultured for 12 and 15 days contain statistical significantly less differentiated BOECs with secondary cilia compared to 23-day culture. Even though 23 day and 6-week BOEC cultures were comparable in confluency, and both presented *in vivo*-like columnar pseudostratified morphology with ciliated and non-ciliated cells, following experiments were performed using the 23-day culture.

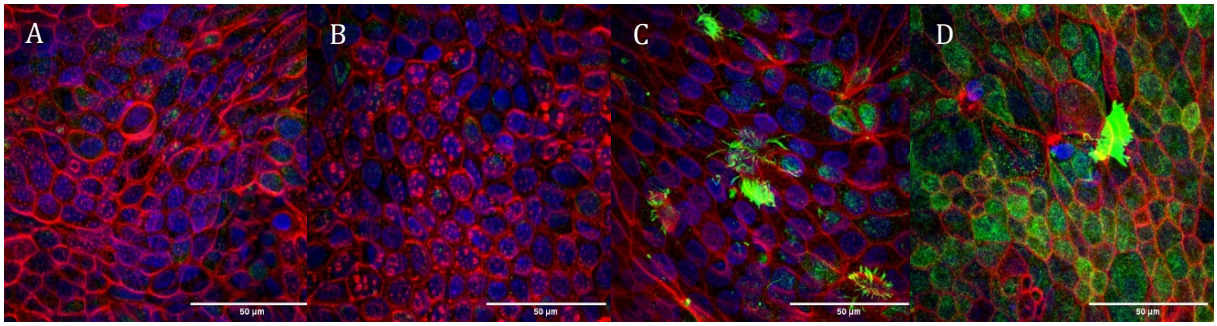

Figure 2: Representative morphology of BOEC monolayers cultured for 12 days (A), 15 days (B), 23 days (C) or 6 weeks (D), stained with phalloidin (red), Hoechst (blue), and anti-acetylated α-tubulin (green). Monolayers cultured for 12 or 15 days showed more irregular morphology, which presented as phalloidin staining in dot patterns at the apical side of the BOECs, compared to 23 days or 6 weeks cultured monolayers.

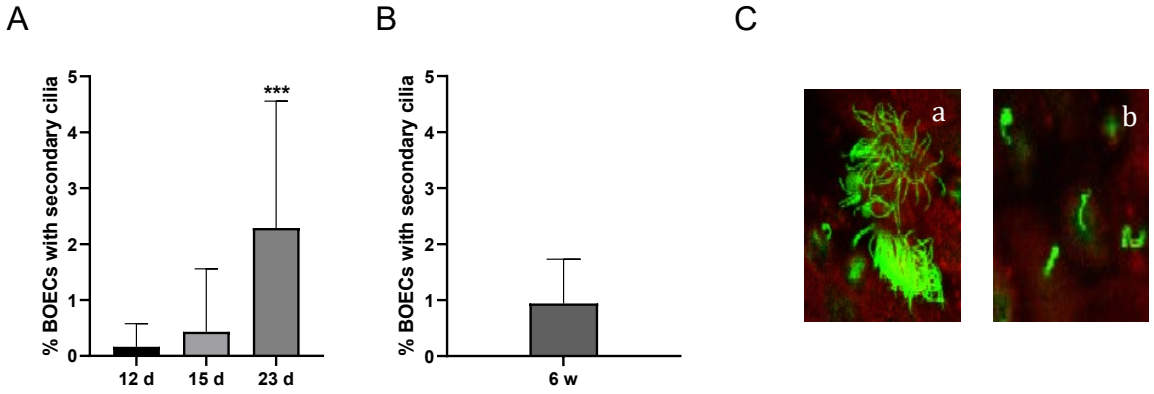

*Figure 3: BOEC monolayers after 12-, 15-, 23 days or 6 weeks of culture in Transwell® inserts. Monolayers of shorter culture duration were established from the same biological material, and the 6-week monolayer from distinct biological material. Bars represent mean ± SD of one replicate. Percentage of BOECs with secondary cilia in BOEC monolayers cultured for 12, 15 or 23 days (A) and monolayers cultured for 6 weeks (B). (C) Image of two secondary cilia (a) and four primary cilia (b). *** Statistically significant difference (P<0.001).*

Pooling material does not affect BOEC differentiation and monolayer confluency

Monolayers used to select BOEC culture duration were established from biological material pooled from four animals. Pooling BOECs from different animal sources could possibly limit differentiation of BOECs to ciliated cells (Chen & Schoen, 2021). Using the 23-day long culture, monolayers were established from material pooled from three animals and compared to monolayers established from single source biologic material (non-pooled, three animals). Monolayers of pooled and non-pooled material were compared on confluency, morphology, and differentiation. Confluency was confirmed by low total percentage of tracer transferred over the BOEC monolayers (<0.5%, Figure 4B) and high TEER values for both non-pooled (1395±55 Ω*cm^2 and 1721±456 Ω*cm^2) and pooled monolayers (1567±240 Ω*cm^2) (Figure 4A). Contrary to this, monolayers established from one of the three non-pooled material never reached the ALI stage, due to leakage of the basolateral media to the apical compartment. Overall, no statistically significant differences in confluency parameters between pooled and non-pooled monolayers were observed. Based on visual observation, there was high variation in the degree of secondary cilia between monolayers established from two distinct single source non-pooled material (Figure 4C-D). Whereas, monolayers established from pooled material (Figure 4E) contained secondary cilia in approximately the same rate as monolayers established from one of the non-pooled material (Figure 4C). This suggests that pooling material from multiple animals does not limit BOEC differentiation and ciliation. Following experiments reported were performed with the use of pooled-source biological material.

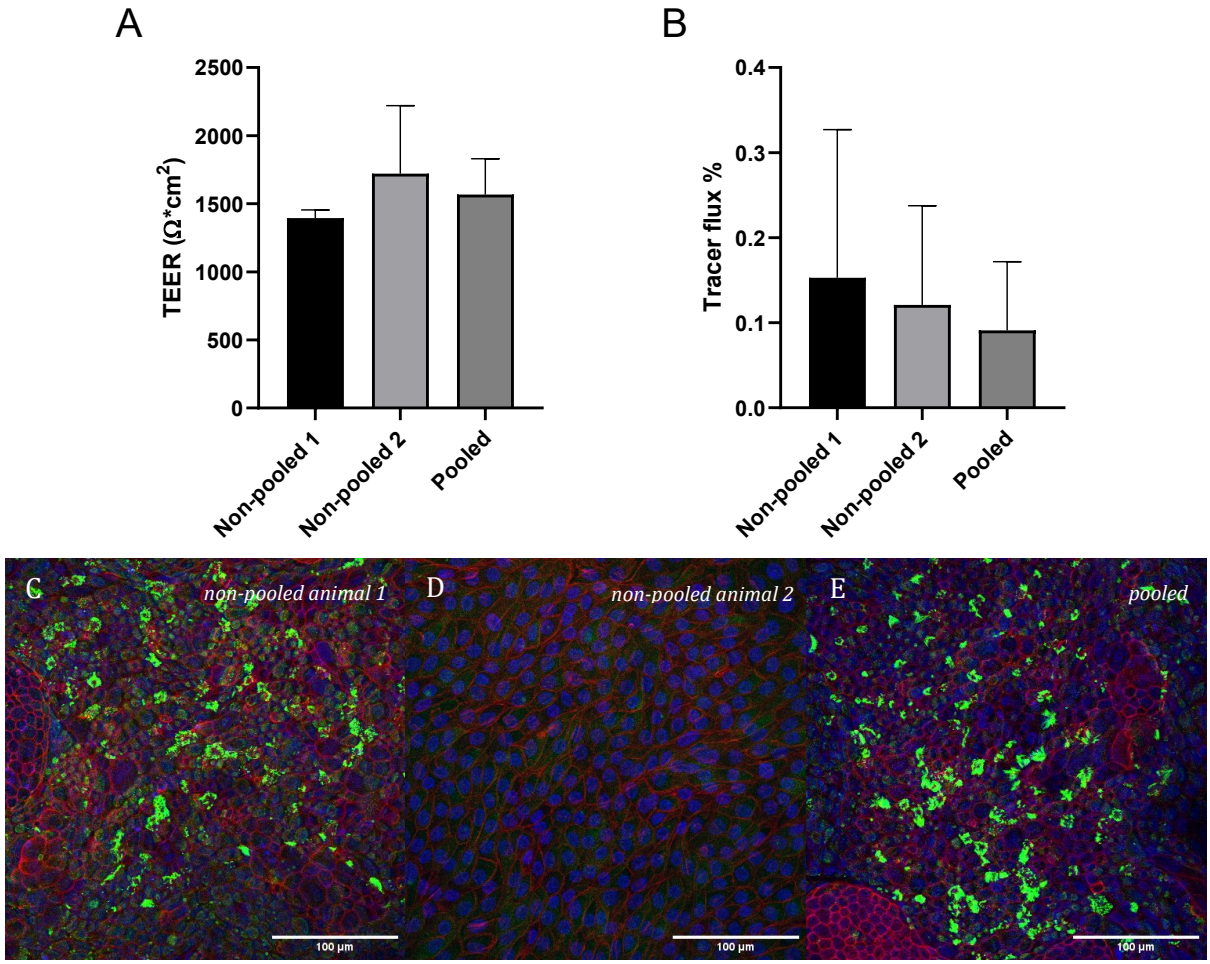

Figure 4: BOEC monolayers established from pooled and non-pooled biological material after 23 days of culture. Confluency was assessed using TEER measurements (A) and percentage tracer flux (B). Bars represent mean ± SD of one replicate. (C-E) Monolayers stained with phalloidin (red), Hoechst (blue), and anti-acetylated α-tubulin (green), (C) monolayer established from non-pooled material animal 1, (D) monolayer established from non-pooled material animal 2, (E) monolayer established from pooled animal.

II. Effect of DES- and KTZ exposure on the BOEC monolayer

DES and KTZ exposure do not affect BOEC viability

First, BOEC viability after DES- and KTZ exposure needed to be determined. Directly after BOEC monolayers were exposed from the basolateral compartment to DES or KTZ (day 23-27), viability was measured using the neutral red assay, which is based on the ability of live cells to retain the neutral red dye in lysosomes. Cell concentration was standardized at the moment of seeding, however after 23 days of culture small variations of monolayer cell concentration could be present. This could present as viability above 100% if the cell concentration of DES- or KTZ treated monolayers were higher compared to the vehicle-treated monolayer. After DES (10^{-9} M, 10^{-7} M, 10^{-5} M) exposure, viability of BOECs was high (98.4%, 96.4%, 100.2%, respectively; Figure 5A), as well as after KTZ (10^{-8} M, 10^{-7} M, 10^{-6} M) exposure (101.8%, 101.2%, 100.0%, respectively; Figure 5B). No statistically significant difference of BOEC viability was observed between different DES and KTZ concentrations. In support of this unaltered BOEC viability, as determined by the neutral red assay, homogeneously stained oval-shaped nuclei with no signs of chromatin condensation or fragmentation were observed after Hoechst 33258 staining (for examples see Figure 5C-E). Thus, exposure to DES and KTZ for four days does not affect BOEC viability.

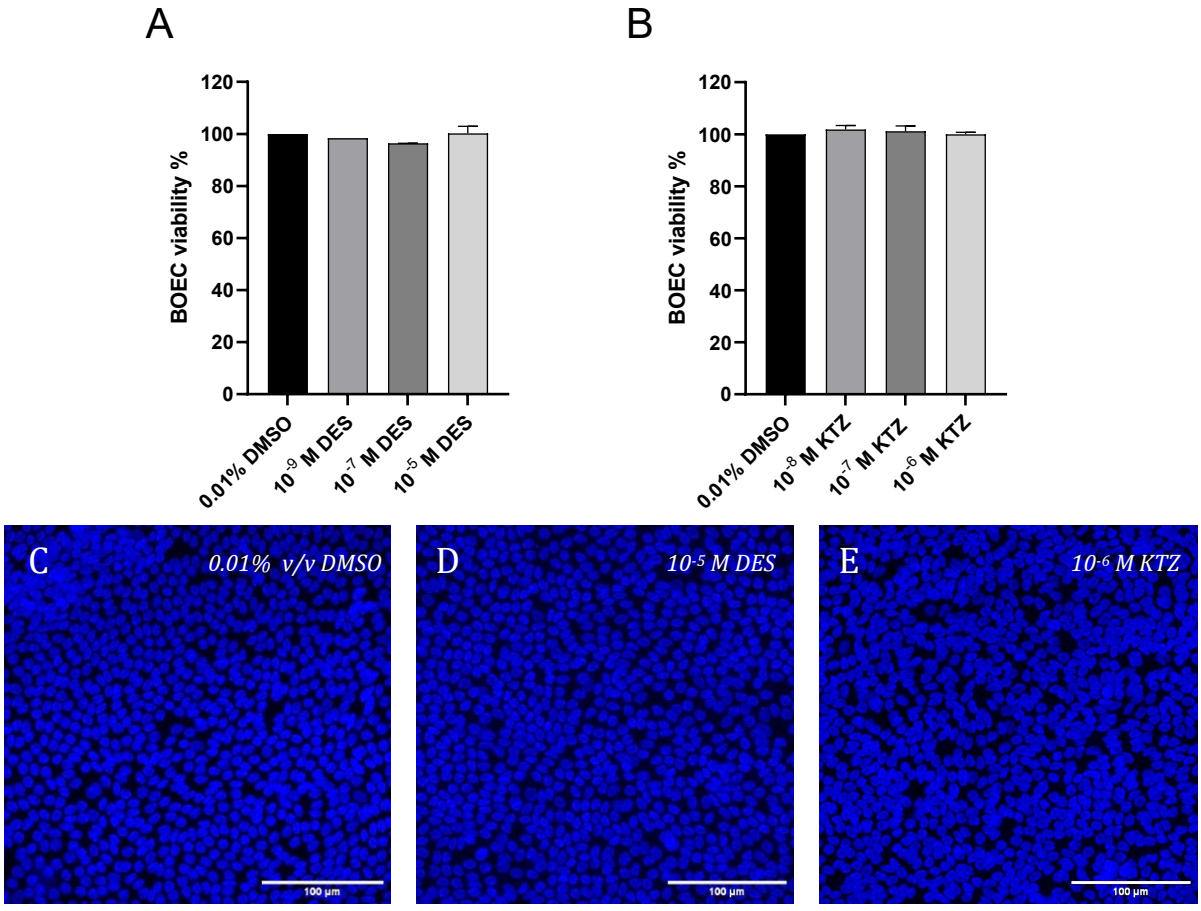

Figure 5: BOEC viability determined after EDC exposure. Cell viability (%) of DES (10^{-9} M, 10^{-7} M, 10^{-5} M) exposed BOEC monolayers (A) and KTZ (10^{-8} M, 10^{-7} M, 10^{-6} M) exposed BOEC monolayers (B), measured with the neutral red assay. Bars represent mean ± SD of one replicate. (C-E) Homogeneous oval-shaped nuclei (blue; Hoechst) after exposure to 0.01% v/v DMSO (C), DES 10^{-5} M (D), KTZ 10^{-6} M (E).

DES and KTZ exposure do not affect monolayer confluency

Exposure to DES or KTZ might alter BOEC monolayer confluency, which was assessed by measuring TEER and tracer flux three days before (day 20) and after (day 27) exposure. At day 20, all monolayers had thus far been cultured under the same conditions, and confluency was confirmed by high TEER (1311±562 $\Omega*cm^2$) and low percentage tracer flux (0.181±0.248 %). BOEC monolayers were exposed (day 23-27) to either DES (10^{-9} M, 10^{-7} M, 10^{-5} M), KTZ (10^{-8} M, 10^{-7} M, 10^{-6} M) or the vehicle (0.01% v/v DMSO) or cultured under normal conditions (control). Control and vehicle-treated BOEC monolayers showed no statistical significant difference in TEER and tracer flux values between day 20 and 27 (Table 1; Figure 6A,E). Contrary, TEER values statistical significantly decreased after exposure to 10^{-7} M and 10^{-5} M DES (1362 vs. 472 $\Omega*cm^2$ and 1425 vs. 430 $\Omega*cm^2$, respectively; Figure 6A) and 10^{-8} M, 10^{-7} M, 10^{-6} M KTZ (1254 vs. 613 $\Omega*cm^2$, 1238 vs. 635 $\Omega*cm^2$, 1245 vs 517 $\Omega*cm^2$, respectively; Figure 6B). Monolayers exposed to the lowest DES concentration (10^{-9} M) did not result in a statistically significant TEER decrease (1347 vs. 746 $\Omega*cm^2$; Figure 6A). However, one 10^{-9} M DES exposed monolayer presented as outlier (out of 8 monolayers; outlier marked in Supplemental table 2), and TEER increased (1347 vs. 746 $\Omega*cm^2$; Figure 6A). When this monolayer was excluded, statistically significant TEER difference after 10^{-9} M DES exposure was determined. Compared to vehicle treated monolayers (-128 $\Omega*cm^2$), TEER decreased significantly after exposure to 10^{-7} M DES, 10^{-5} M DES and 10^{-7} M KTZ (-889 $\Omega*cm^2$, -995 $\Omega*cm^2$, -603 $\Omega*cm^2$, respectively; Figure 6C-D). Regardless of decreasing TEER values after DES- or KTZ exposure, values still supported confluency. This was substantiated by TEER values of non-confluent monolayers (8 ± 7 $\Omega*cm^2$). The low TEER values of non-confluent monolayers were accompanied by high tracer flux percentage (15±2%), which were comparable to tracer flux percentage of empty control inserts without BOECs (17±8%) (Figure 7). Regarding paracellular transport, there was low percentage (≤0.8%) of total tracer transferred from the apical to the basolateral compartment in all monolayers, with a slightly higher percentage in three single monolayers: 1.57% (0.01% v/v DMSO), 1.20% (10^{-7} M KTZ), and 1.52% (10^{-5} M DES). No statistically significant difference in total tracer transfer before and after exposure to all DES and KTZ concentrations was observed (Figure 6E-F). Additionally, there was no statistically significant difference in change of percentage tracer flux (from day 20 to 27) between DES- and KTZ exposed monolayers vs. vehicle-treated monolayers (Figure 6G-H). In addition, confluency was also assessed using confocal microscopy. Monolayers were stained against F-actin (phalloidin), and clear basolateral cell-cell interaction, as well as cell-membrane adhesion was observed for all monolayers. Consequently, this suggests that four-day exposure to DES or KTZ, at all tested concentrations, does not alter BOEC monolayer confluency.

Table 1: Average values of confluency parameters (TEER $\Omega*cm^2$ and tracer flux %) before and after DES (10^{-9} M, 10^{-7} M, 10^{-5} M), KTZ (10^{-8} M, 10^{-7} M, 10^{-6} M), or vehicle (0.01% DMSO) exposed monolayers, as well as change in values. Values of individual monolayers are reported in Supplemental table 2.

	TEER ($\Omega*cm^2$)			**Tracer flux %**		
	Before	**After**	**Change**	**Before**	**After**	**Change**
Control	1310	1116	-193	0,19%	0,18%	-0,01%
0.01% v/v DMSO	1326	1198	-128	0,45%	0,16%	-0,30%
10^{-9} M DES	1346	746	-601	0,17%	0,19%	0,02%
10^{-7} M DES	1362	472	-889	0,19%	0,23%	0,03%
10^{-5} M DES	1425	430	-995	0,10%	0,39%	0,26%
10^{-8} M KTZ	1254	613	-642	0,16%	0,34%	0,18%
10^{-7} M KTZ	1238	635	-603	0,11%	0,37%	0,26%
10^{-6} M KTZ	1245	517	-640	0,09%	0,19%	0,10%

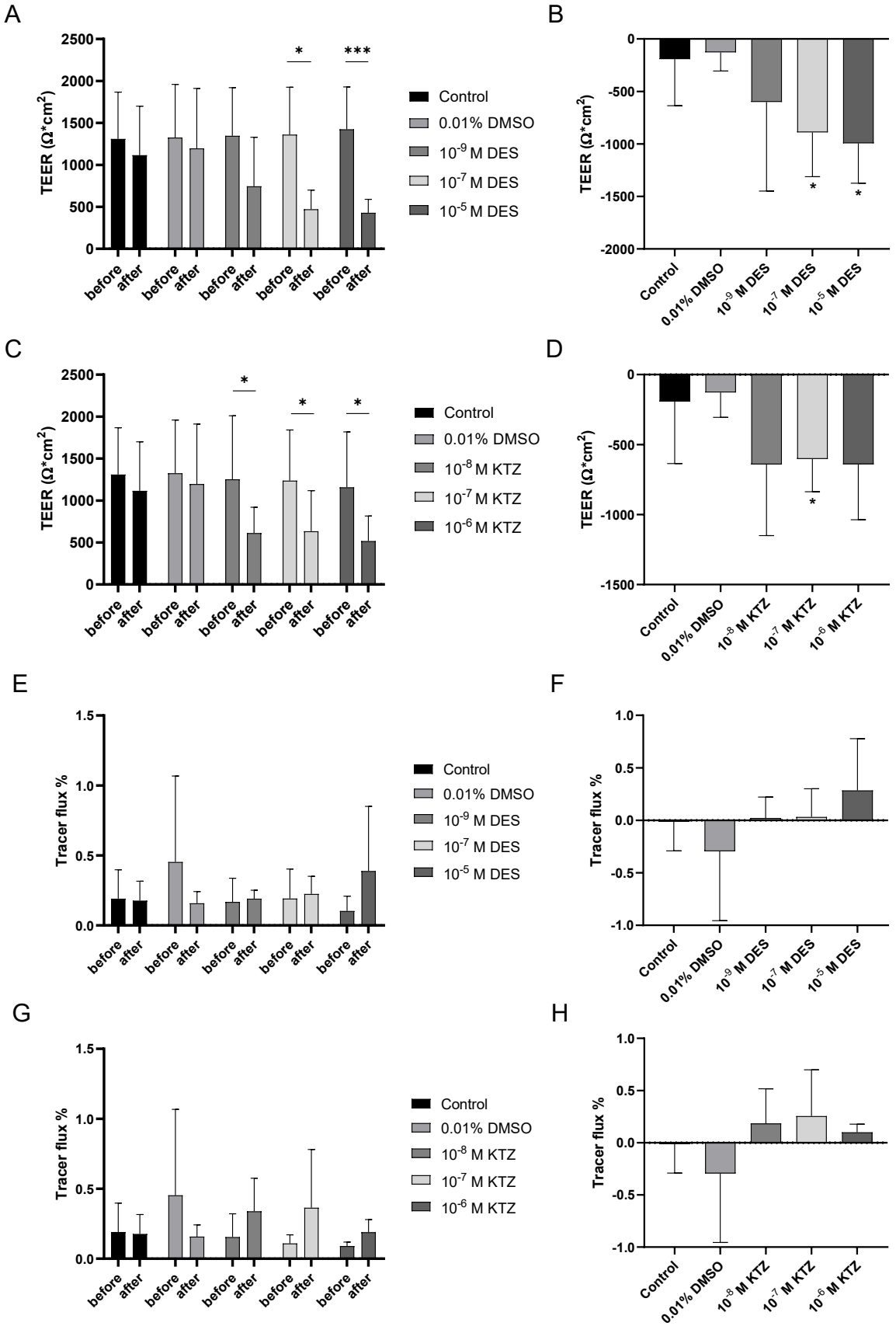

*Figure 6: Confluency assessment of BOEC monolayers after DES and KTZ exposure, using TEER and tracer flux measurement. Bars represent mean ± SD of three replicates. (A-D) TEER values before and after DES exposure (A) and KTZ exposure (C), as well as change in TEER values after DES (B) and KTZ (C). (E-H) Percentage tracer flux before and after DES exposure (E) and KTZ exposure (G), as well as change in tracer flux % after DES (F) and KTZ (H) exposure. Statistical significance * (P<0.05) and *** (P<0.001).*

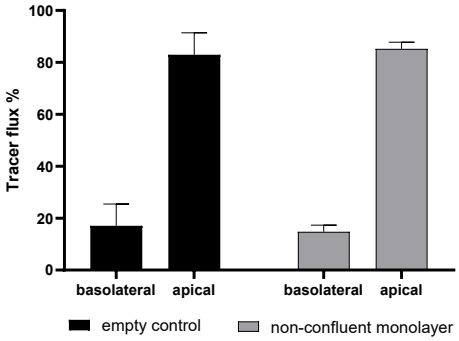

*Figure 7: Percentage tracer in basolateral and apical compartment of empty control inserts (without BOECs), and non-confluent monolayers. Empty control 17±8%, non-confluent monolayer 15±2%: Average TEER value of these non-confluent monolayers was 8 ± 7 Ohm * cm². Bars represent mean ± SD*

BOEC differentiation to ciliated cells is decreased after DES- and KTZ exposure

Besides the monolayer confluency, a parameter of BOEC monolayer integrity after DES and KTZ exposure, the differentiation of BOECs to ciliated cells was also assessed. Overall low percentage of BOECs with secondary cilia was observed, where control and vehicle-treated monolayers contained an average of 0.8±1.4% and 2.2±3.5% BOECs with secondary cilia, respectively (Figure 8A-B). Secondary cilia were observed to localise in clusters, rather than equally dispersed throughout the monolayer (see Figure 8C-D for examples). The highest percentages reported were 11.7% and 9.9% in vehicle-treated monolayers, while other areas of the same monolayer did not present any secondary cilia (values of individual monolayers see Supplemental table 3). However, monolayers exposed to the lowest and middle DES concertation (10^{-9} M and 10^{-7} M) displayed statistically significant less BOECs with secondary cilia (0.1±0.2% and 0.2±0.6%) compared to control and vehicle-treated monolayers (Figure 8A). Similarly, 10^{-8} M and 10^{-6} M KTZ treated monolayers displayed statistically significant less secondary cilia (0.2±0.6% and 0.2±0.4%) compared to control monolayers, but no statistically significant difference compared to vehicle-treated monolayers was observed (Figure 8B). Monolayers exposed to 10^{-5} M DES and 10^{-7} M KTZ did not display statistically significant less BOECs with secondary cilia (0.3±0.6% and 0.3±0.7%, respectively) compared to control and vehicle-treated monolayers. In conclusion, BOEC monolayers exposed to DES (10^{-9} M, 10^{-7} M) and KTZ (10^{-8} M, 10^{-6} M) show a statistically significant lower percentage of BOECs with secondary cilia. Nonetheless, the degree of BOECs with secondary cilia were generally low, even in control BOEC monolayers (0.8±1.4%).

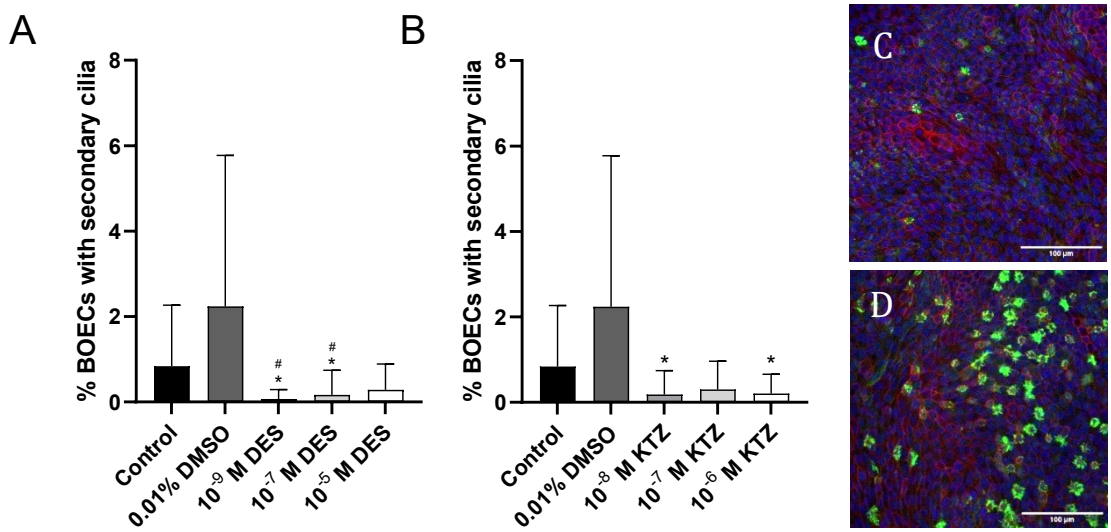

*Figure 8: Secondary cilia presenting on the apical side of BOEC monolayers. (A-B) Percentage of BOECs with secondary cilia after DES exposure (A) or KTZ exposure (B). Bars represent mean ± SD of three replicates. (C-D) Secondary cilia in BOEC control (C) and vehicle -treated (D) monolayers. * Statistically significant different to control monolayers (P<0.05). # Statistically significant different to vehicle-treated (P<0.05).*

Lowered lateral cell-cell adherence position after DES- and KTZ exposure

Contrary to the previously reported clear basolateral cell-cell adherence as well as cell membrane adherence (see section: DES and KTZ exposure does not affect monolayer confluency), a lowered position of lateral cell-cell adherence was observed in a subpopulation of BOECs after DES or KTZ exposure. The altered lateral cell-cell adherence presented as detached cytoskeleton patterns between cells, visualised using phalloidin (F-actin) staining, and increased in distance towards the apical side of the BOECs. Occurrence of this lowered position of lateral cell-cell adherence was not diffuse throughout the monolayer. Some areas presented tight apical lateral cell-cell adherence (Figure 9A-B), whereas, in other areas there was high occurrence of a more basolateral position of lateral cell-cell adherence and can be clearly seen in the orthogonal and 3D view (Figure 9A-B). To compare the degree of lowered position of lateral cell-cell adherence, phalloidin patterns were categorized based on the quantity of lowered position of lateral cell-cell adherence. Five categories were made, ascending in the quantity of lowered lateral position of cell-cell adherence. Representative images of the basal side, in the middle, and the apical side of the monolayers are depicted in Figure 10. Categories: (0) no altered adherence between BOECs present (Figure 10A); (1) up to ~5% lowered lateral position of cell-cell adherence between BOECs (Figure 10B); (2) up to 50% lowered lateral position of cell-cell adherence between BOECs (Figure 10C); (3) around 75% lowered lateral position of cell-cell adherence between BOECs (Figure 10D); (4) ≥75% lowered lateral position of cell-cell adherence between BOECs (Figure 10E). High statistically significant difference of lowered lateral position of cell-cell adherence after DES- (10^{-9} M, 10^{-7} M, 10^{-5} M; Figure 11A) and KTZ- (10^{-8} M, 10^{-7} M, 10^{-6} M; Figure 11B) exposed vs. control and vehicle-treated monolayers was observed ($P<0.001$). Furthermore, BOECs in areas with lowered lateral position of cell-cell adherence still present a columnar phenotype, indicated by height-width ratio. Apparently, four-day exposure of DES and KTZ from the basolateral side, allows movement of the apical to a more basal position of lateral cell-cell adherence in BOEC monolayers.

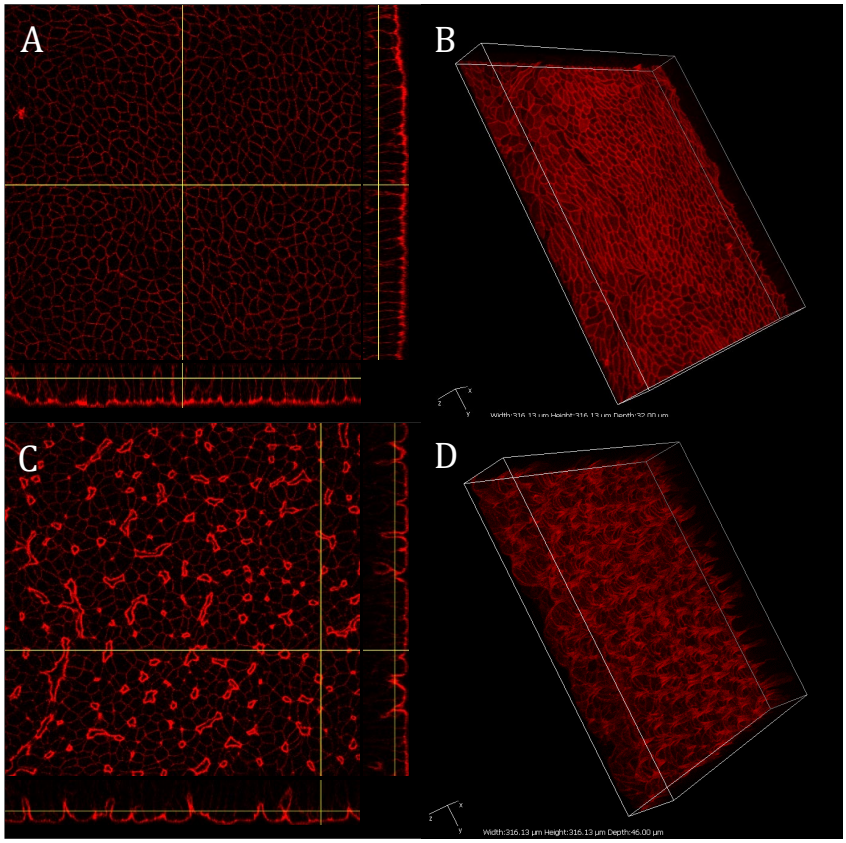

Figure 9: Altered lateral cell-cell adherence in BOEC monolayers after DES- and KTZ exposure. (A-D) Monolayers present tight apical lateral cell-cell adherence shown by orthogonal view (A) and 3D view (B). Monolayers present more basal lateral cell-cell adherence position shown in orthogonal view (C) and 3D view (D).

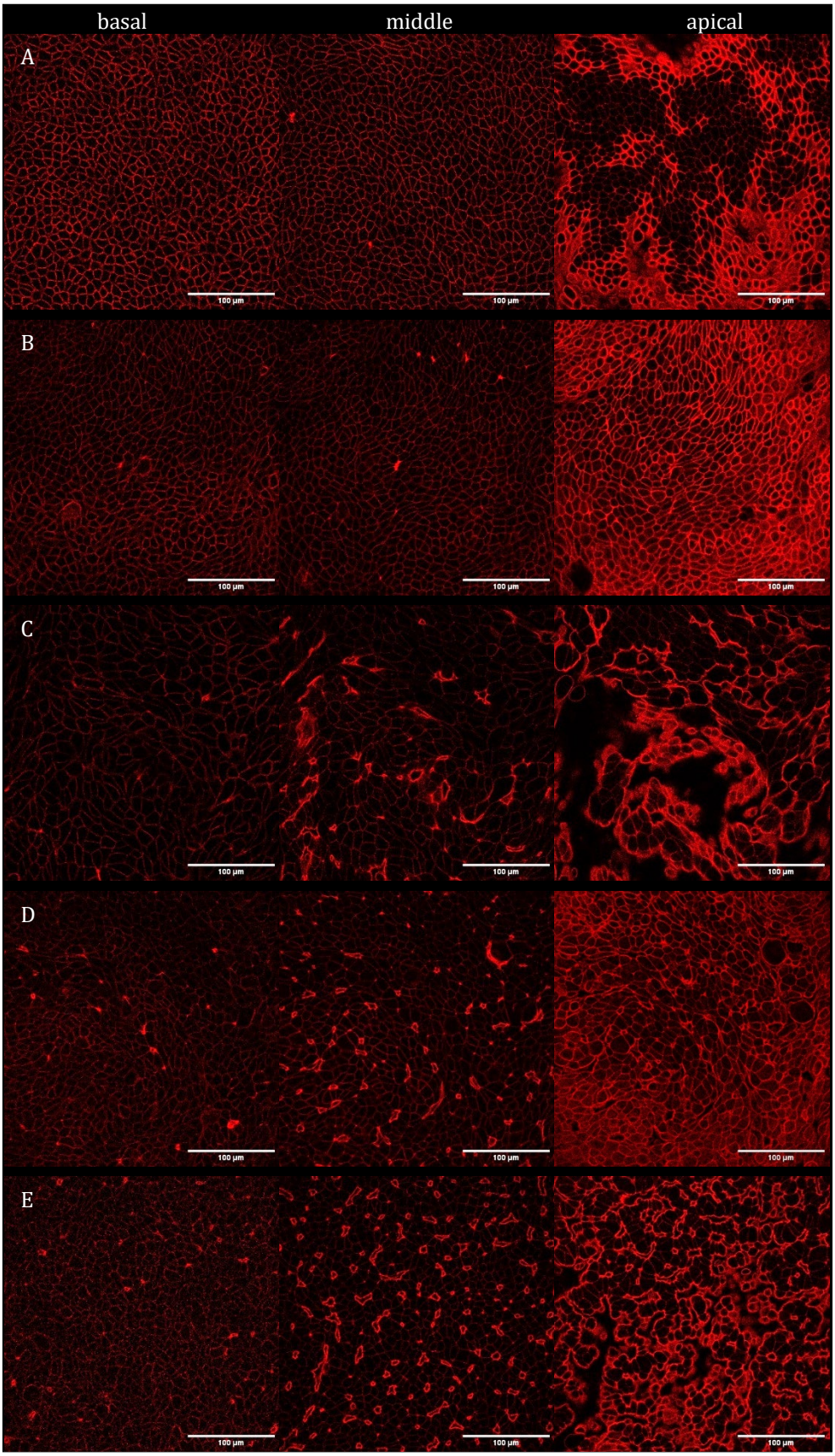

Figure 10: Representable images of categories of lowered lateral position of cell-cell adherence between BOECs visualized by phalloidin (red). Three images of the z-stack are depicted, basal side of the monolayer, in the middle of the monolayer, and the apical side of the monolayer. (A) category 0; consists of no altered position of lateral cell-cell adherence between BOECs, (B) category 1; 0-5% lowered position of lateral cell-cell adherence between BOECs, (C) category 2; up to ~50% lowered position of lateral cell-cell adherence between BOECs, (D) category 3; around 75% lowered position of lateral cell-cell adherence between BOECs, (E) category 4; ≥75% lowered position of lateral cell-cell adherence between BOECs.

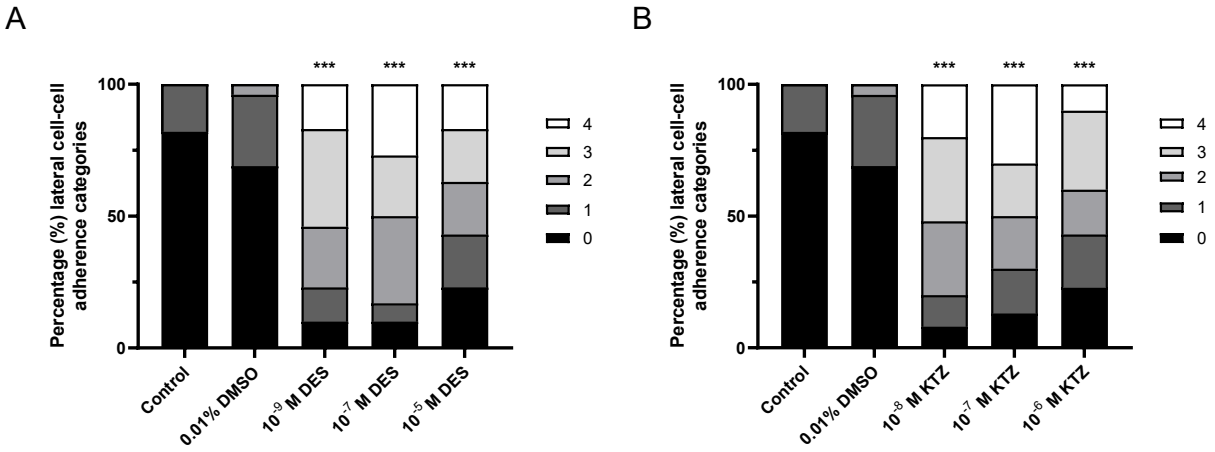

*Figure 11: Percentual frequency of lowered lateral position of cell-cell adherence between BOECs (categorized 0-4). (A) DES (10^{-9} M, 10^{-7} M, 10^{-5} M) exposed monolayers and (B) KTZ (10^{-8} M, 10^{-7} M, 10^{-6} M) exposed monolayers. Based on three individual replicates. Categories; 0: no lowered position of lateral cell-cell adherence, 1: up to ~5% lowered position of lateral cell-cell adherence, 2: up to 50% lowered position of lateral cell-cell adherence, 3: up to 75% lowered position of lateral cell-cell adherence, 4: >75% lowered position of lateral cell-cell adherence. Representative images of the categories see Figure 10. Values of individual monolayers see Supplemental table 3. *** Statistical significance (P<0.001).*

Change in TEER from day 20 to day 27 (Table 1) has an inverse statistically significant correlation with the degree of lowered position of lateral cell-cell adherence between BOECs (r= -0.33, P<0.05). Contrary, the change in percentage tracer transferred over BOEC monolayers has a statistically significant correlation with the degree of lowered position of lateral cell-cell adherence between BOECs (r = 0.30, P<0.05). As expected, the correlation of TEER and percentage tracer flux with the degree of lowered position of lateral cell-cell adherence is inverse (r= -0.33 and r = 0.30, respectively).

Recovery after DES exposure

To test whether effects caused by DES (10^{-9} M, 10^{-7} M, 10^{-5} M) exposure on BOEC monolayers were reversible, monolayers were cultured for four days under normal conditions after a four-day exposure period. Confluency was measured three days before exposure (day 20), after exposure (day 27) and after recovery (day 31), using TEER and tracer flux. Statistical significance was not tested since data were obtained from one replicate. After exposure to DES (10^{-9} M, 10^{-7} M, 10^{-5} M) TEER values decreased. Monolayers exposed to 10^{-9} M and 10^{-7} M DES showed increased TEER values after a recovery period, 1814 vs. 664 vs. 2242 Ω*cm^2 and 1962 vs. 484 vs. 1903 Ω*cm^2, respectively (Figure 12A). Contrary to this, monolayers exposed to highest DES concentration (10^{-5} M) showed a substantial lower increase after recovery, 1937 vs. 593 vs. 930.6 Ω*cm^2 (Figure 12A). TEER values after recovery were more comparable to values obtained before exposure, suggesting that the effect by DES was reversible. Like previously mentioned (see section: DES and KTZ exposure does not affect monolayer confluency), tracer flux values remained low not only before but also after DES (10^{-9} M, 10^{-7} M, 10^{-5} M) exposure, similarly, values remained low after recovery period (0.10 vs. 0.25 vs. 0.07%, 0.18 vs. 0.18 vs. 0.11 %, 0.21 vs. 0.20 vs. 0.15 %, respectively; Figure 12B). As previously mentioned, BOECs showed altered morphology after DES exposure: they displayed a statistically significant lowered position of lateral cell-cell adherence (Figure 9E). After a four day recovery period, the middle and highest DES concentration (10^{-7} M, 10^{-5} M) showed decrease in occurrence of lowered position of lateral cell-cell adherence between BOECs, whereas 10^{-9} M DES exposed monolayers after a recovery period showed a similar degree of lowered position of lateral cell-cell adherence compared to after exposure (Figure 13). However, presence of lowered cell-cell adherence after a four-day recovery period was still substantially higher compared to control and vehicle-treated monolayers at day 27 of culture (Figure 9A). Further, the percentage of BOECs with secondary

cilia was low in monolayers treated with DES (10^{-9} M, 10^{-7} M, 10^{-5} M), as well as in control and vehicle-treated monolayers (Figure 8A). Monolayers recovered after DES exposure (10^{-9} M, 10^{-7} M, 10^{-5} M) contained little to no secondary cilia (0%, 0%, 0.18%, respectively). It appeared that, after DES exposure TEER values decreased substantially, however confluency was maintained. When exposed monolayers were allowed to recover for four days, the values of confluency parameter TEER were increased and were comparable to values recorded prior to exposure. However, it seems like the effects on the lateral cell-cell adherence and degree of secondary cilia caused by DES exposure was not reversible after a four-day recovery period.

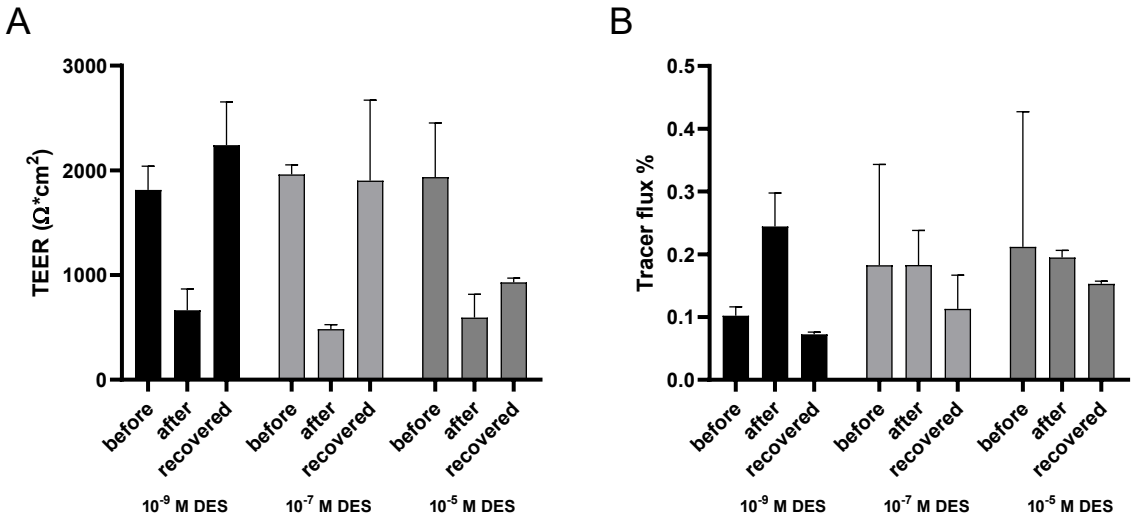

Figure 12: Confluency parameters of BOEC monolayer before exposure, after four-day DES (10^{-9} M, 10^{-7} M, 10^{-5} M) exposure, followed by a four-day recovery period. (A) TEER values. (B) Percentage tracer flux. (before: day 20, after: day 27, recovered: day 31). *Bars represent mean ± SD of one replicate.*

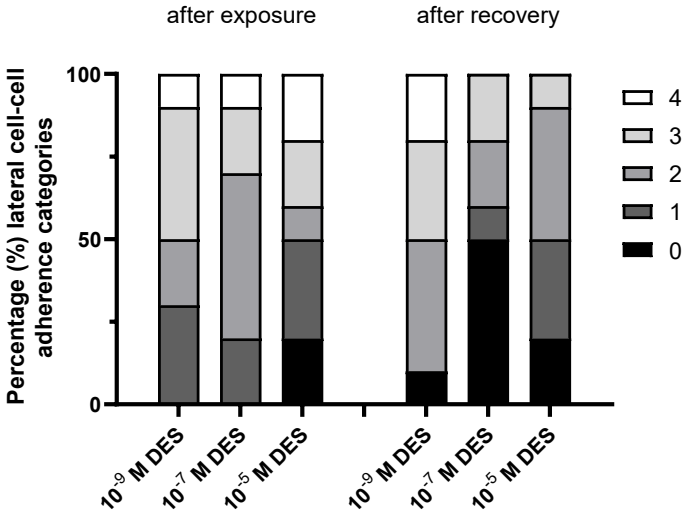

Figure 13: Percentual frequency of lowered position of lateral cell-cell adherence between BOECs (categorized 0-4) in monolayers after DES (10^{-9} M, 10^{-7} M, 10^{-5} M) exposure (after exposure), and in monolayers cultured for a four-day recovery period after DES (10^{-9} M, 10^{-7} M, 10^{-5} M) exposure (after recovery). Based on one replicate. Categories; 0: no lowered position of lateral cell-cell adherence, 1: up to ~5% lowered position of lateral cell-cell adherence, 2: up to 50% lowered position of lateral cell-cell adherence, 3: up to 75% lowered position of lateral cell-cell adherence, 4: >75% lowered position of lateral cell-cell adherence. Representative images of categories see Figure 10.

III. Embryo co-culture in the BOEC-ALI model

Apical synthetic oviductal fluid (SOF) incubation does not affect monolayer confluency and BOEC differentiation

For embryo co-culture in the BOEC-ALI system, first the effect of embryo culture media (i.e., SOF) on the BOEC monolayer needed to be assessed. SOF was incubated from day 23-27 (which was parallel to day 1-5 of *in vitro* embryo culture; IVP) on the apical side of the BOEC monolayer. BOEC monolayers cultured with 50 µl or 150 µl SOF in the apical compartment did not present altered confluency. Surprisingly, 100 µl SOF resulted in statistically significant increase of TEER values (1345 vs. 2505 Ω*cm^2), compared to ALI control monolayers (1263 vs. 1285 Ω*cm^2) (Figure 14A). The total percentage paracellular tracer transfer over the monolayer was low (<0.7%) in SOF incubated and control monolayers (Figure 14B). When BOEC morphology and differentiation were assessed, SOF incubation at the apical compartment of the BOEC monolayer did not induce any changes, compared to ALI control monolayers. Specifically, BOECs with secondary cilia occurred to the same extend regardless of SOF volume (50 µl, 100 µl, 150 µl; 1.34±1.64%, 0.73±1.19%, 0.99±1.41%, respectively vs. 0.84±1.42% control) (Figure 14C). Furthermore, no changes in lateral position of cell-cell adherence were observed. This may suggest that four-day apical SOF culture does not induce dedifferentiation of the BOECs or induced changes in confluency of the monolayer and/or lateral cell-cell adherence.

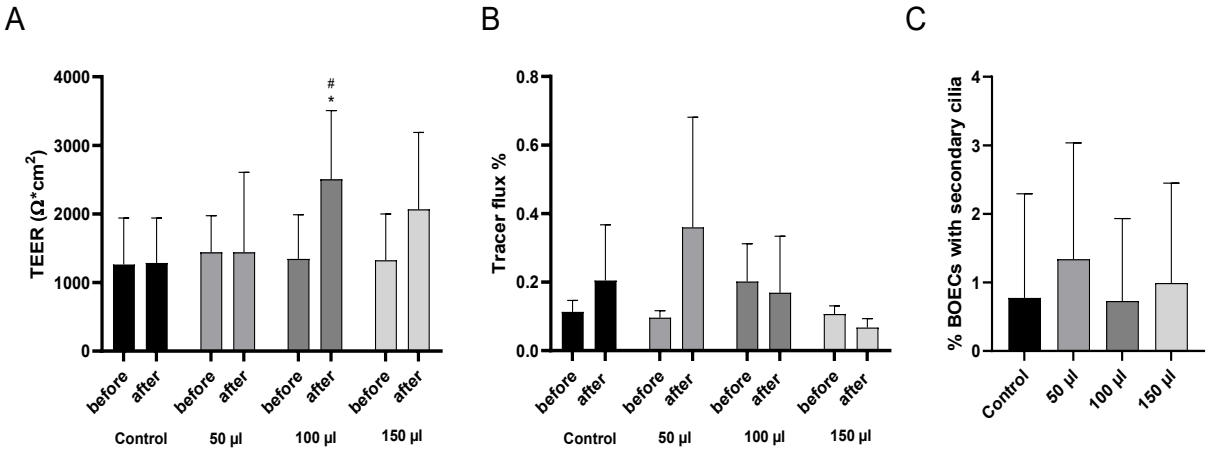

*Figure 14: Four-day incubation of SOF in apical compartment, where control was monolayer with empty apical compartment. Bars represent mean ± SD of two replicates. (A) TEER measurement and after SOF incubation. (B) Percentage tracer flux in basolateral compartment before and after apical SOF incubation. (C) Percentage secondary cilia (mean ± SD) after SOF incubation. Statistical significance * compared to before (P<0.05), # compared to control monolayer (P<0.05).*

In vitro embryo co-culture in the BOEC-ALI system does not produce blastocysts

After determining that apical SOF incubation does not affect BOEC monolayers, embryo co-culture was performed. Presumed zygotes were produced by *in vitro* maturation (IVM) of bovine oocytes and subsequent *in vitro* fertilization (IVF). The presumptive zygotes were then used for *in vitro* embryo culture (IVC) in SOF in the apical compartment of the BOEC-ALI system for four days. Groups of presumed zygotes in different numbers (6, 15, 30) and SOF volumes (100 µl, 150 µl) were tested for optimum blastocyst development, one replicate with duplicate of each group. Embryo cleavage rate was recorded at day 5, they were then transferred to the normal IVC system (see methods; BOEC air-liquid interface culture, embryo co-culture), and blastocyst rate was recorded at day 7 and 8 (Table 2). Presumed zygotes co-cultured in BOEC-ALI showed lower cleavage rate compared to presumed zygotes cultured according to the standard IVC procedure (control). The highest cleavage was achieved when 6 or 15 presumed zygotes were cultured in

100 µl SOF, 61% and 59%, respectively. Only co-culture under these conditions produced blastocysts, 9% (6 zygotes, 100 µl SOF) and 3% (15 zygotes, 100 µl SOF). Although, these percentages represent only one blastocyst formed in either culture conditions. In parallel, the standard IVP procedure was carried out (control), with a recorded day 8 blastocyst rate of 34%, which is considered a normal blastocyst yield for this IVP protocol (30-40% blastocyst rate expected).

Table 2: Day 5 cleavage rate and Blastocyst rate at day 7 and 8 of IVP in apical compartment of BOEC monolayers. Control was standard IVP procedure. Based on one replicate, duplicate per group.

	Control	6 zygotes 100 µl	6 zygotes 150 µl	15 zygotes 100 µl	15 zygotes 150 µl	30 zygotes 100 µl	30 zygotes 150 µl
d 5 cleavage %	76	61	42	59	28	51	21
d 7 blastocyst %	25	9	0	3	0	0	0
d 8 blastocyst %	34	9	0	3	0	0	0

BOEC monolayer confluency was not altered after co-culture, confirmed by low percentage (<0.6%) of total tracer transferred over BOEC monolayer, and high TEER values. BOECs maintained lateral cell-cell adherence, in a comparable manner to monolayers cultured without presumed zygotes (Figure 15A). However, after presumed zygotes were co-cultured, the percentage of BOECs with secondary cilia was decreased compared to empty control monolayers (Figure 15B). This could suggest that co-culture of presumed zygotes induces dedifferentiation of BOECs.

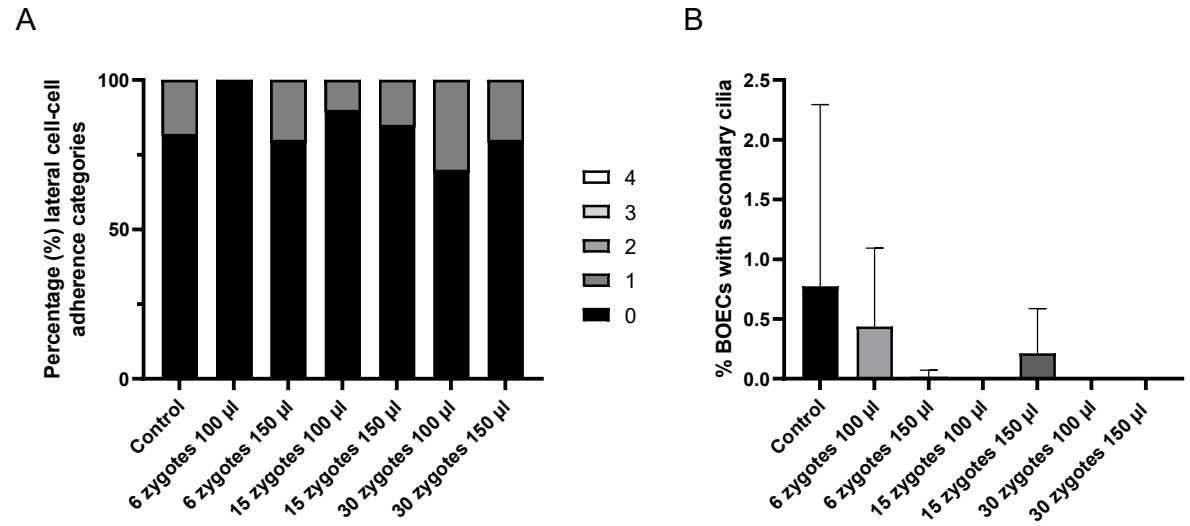

Figure 15: In vitro embryo production (IVP) performed in the apical compartment of BOEC monolayers, where control was monolayer in ALI stage. Bars represent± SD of one replicate. (A) Percentual frequency of lowered lateral cell-cell adherence between BOECs (categorized 0-4) in monolayers after IVP in the apical compartment of BOEC monolayers. Categories; 0: no lowered position of lateral cell-cell adherence, 1: up to ~5% lowered position of lateral cell-cell adherence, 2: up to 50% lowered position of lateral cell-cell adherence, 3: up to 75% lowered position of lateral cell-cell adherence, 4: >75% lowered position of lateral cell-cell adherence. Representative images of categories see Figure 10. (B) Percentage BOECs with secondary cilia.

Discussion

The increase of female reproductive disorders is considered to be partially related to the rise in endocrine disrupting chemicals (EDCs) production and exposure (Delbes et al., 2022; Ding et al., 2020; Ma et al., 2019). However, there is minimal research about the impact of EDCs on the oviduct, the site of oocyte fertilization and early embryonic development, reported. Here, we tested the effect of two classic EDCs diethylstilbestrol (DES; a synthetic estrogen agonist) and ketoconazole (KTZ; a steroidogenic enzyme inhibitor) on the oviduct epithelium. For this purpose, we employed the bovine oviduct epithelial cell (BOEC) air-liquid interface (ALI) culture as a suitable model for (in)direct EDC exposure and embryo co-culture. The bovine was used for this model since early bovine embryos have been reported to be comparable to human embryos in the preimplantation period and are widely used as human IVF models (Ménézo & Hérubel, 2002; Santos et al., 2014). Here, we optimized a BOEC-ALI culture by adopting a culture duration of 23-days, established from pooled biological material. BOECs were differentiated with an *in vivo*-like columnar epithelial phenotype consisting of ciliated and non-ciliated cells. Four-day exposure to DES (10^{-9} M, 10^{-7} M, 10^{-5} M) or KTZ (10^{-8} M, 10^{-7} M, 10^{-6} M) did not affect BOEC viability and BOEC monolayer confluency, indicating that this model is suitable for EDC exposure.

In the *in vivo* bovine oviduct ciliated cells constitute 40-70% of total epithelial cells, depending on the location in the oviduct and the phase of the estrous cycle (Abe & Oikawa, 1993; Lyons et al., 2002). Cilia play an important role in reproduction, such as for the active transport of gametes and embryos. To mimic the *in vivo* oviduct physiology, BOECs in ALI culture should differentiate to ciliated cells. Here, the 23-day BOEC-ALI culture contained an overall low percentage of secondary cilia (0.8±1.4%), and the primary cilia were not analysed due to time limitations. Unfortunately, the degree of ciliation observed in this culture does not mimic the *in vivo* situation. The secondary cilia were observed to be localized predominantly in clusters, rather than a disperse distribution throughout the monolayer, and this phenomenon was also observed in a previously established 9-day long BOEC-ALI culture (Jordaens et al., 2015). At first, we hypothesized that pooling biological material could inhibit BOEC differentiation and therefore reduce the degree of ciliation (Chen & Schoen, 2021). Contradictory to our assumptions, monolayers established from distinct individual non-pooled material showed high variation in the degree of secondary cilia, while monolayers established from the combined material (pooled) showed ciliation comparable to one of the individual non-pooled material monolayers. This suggests that the degree of ciliation is dependent on the animal. It is known that around ovulation and during the follicular phase when 17β-estradiol (E2) production is high, the oviduct epithelium is predominated by ciliated cells (Abe & Oikawa, 1993; Yániz et al., 2000). Exogenous E2 administration from the basolateral compartment has shown to increase the degree of ciliation in a porcine OEC-ALI and BOEC microfluidic chip system (Chen et al., 2013a; Ferraz et al., 2018). Considering the data above, it is possible that BOECs isolated from cattle at the follicular phase may develop more cilia in an ALI culture. For our established BOEC-ALI cultures the estrous cycle phase was determined (Supplemental table 4). Another aspect of our ALI protocol that is distinct from other OEC-ALI cultures, which achieved differentiated OECs with normal morphology and secondary cilia, is the seeding method. We use an indirect seeding method to eliminate fibroblasts, while other studies used a direct seeding protocol and implemented another way for fibroblast removal (Chen et al., 2017; Chen & Schoen, 2021; Jordaens et al., 2015; Leemans et al., 2022). Direct seeding could potentially maintain secondary cilia of the isolated OECs. Additionally, the degree of ciliation could possibly be increased by coating the membrane of the inserts with extracellular matrix proteins, to increase polarization of the BOECs. For porcine and mice OEC-ALI membrane coating with collagen type IV has been reported (Chen et al., 2017). Lastly, in our effort to increase ciliation we extended the culture timing to 6 weeks to allow more time for BOEC differentiation, but we observed no difference compared to shorter culture duration (23-days). However, if one of the previously mentioned suggestions for increased ciliation is implemented, the culture duration could be re-evaluated.

After the BOEC-ALI culture was established, it was used as a toxicological model to test the effect of the EDCs DES and KTZ on the BOECs. Exposure to DES (10^{-9} M, 10^{-7} M, 10^{-5} M) or KTZ (10^{-8} M, 10^{-7} M, 10^{-6} M) for four days did not alter BOEC viability and monolayer confluency. Although clear basolateral cell-cell and cell-membrane attachment was observed, there was lowered position of lateral cell-cell adherence between the BOECs, accompanied by significantly decreased TEER values, while confluency is not affected. TEER measures the paracellular ionic conductance over epithelial monolayers, and this can be used to study epithelial barrier integrity and the integrity of cell-cell junctions. For instance, tight junctions can resist paracellular ionic flow and thereby increase the resistance over the epithelial monolayer (Anderson, 2001; Chen et al., 2015; Srinivasan et al., 2015). The observed lowered position of lateral cell-cell adherence could be explained as a transfer of the cell-cell contact zone, to a more basal localization, where the contact zone is not functionally altered. By decreasing the distance between the basolateral media and apical media, the ionic conductance can increase and subsequently decrease the TEER values. Another explanation for the lowered position of lateral cell-cell adhesion could be an alteration of cell-cell junction proteins *e.g.,* tight junction proteins. Multiple studies have reported the effect of estrogen exposure on the remodelling of tight junctions (Zeng et al., 2004). It is suggested that exposure of epithelial cells to estrogen induces proteolysis of occludin (Zhu et al., 2006) and this effect is mediated through the nuclear estrogen receptor alpha (ERα) (Gorodeski, 2007; Gorodeski & Pal, 2000). In support of this, *in vitro* cultured epithelial cells exhibited a decreased transepithelial resistance after two-day estrogen (E2) exposure from both the basolateral and the apical side (Zeng et al., 2004). Like physiological estrogen, DES mediates its effect through ERα (Bolger et al., 1998). Additionally, the effects of DES on the cytoskeleton have been described in literature. Increased acetylation levels of α-tubulin have been reported in the oocyte, which leads to microtubule stabilization after DES exposure (Ding et al., 2020). Further, DES is a calcium channel blocker, and exposure to DES leads to calcium dependent destabilization of actin filaments (Janevski et al., 1993). Cytoskeleton components are strongly associated with cell-cell adhesion (Hoelzle & Svitkina, 2012). Interestingly, KTZ showed the same effect of lowered lateral position of cell-cell adherence as DES. Compared to estrogens, there is little reported about the effect of azoles on the cell-cell contact zone and cytoskeleton. A previous study showed that *in vivo* exposure of fluconazole, another potent EDC from the azole family like KTZ, in mice resulted in a decreased expression of tight junctions proteins occludin and ZO-1 in colon epithelia (Qiu et al., 2016). Additionally, KTZ is known to act as an androgen receptor antagonist, a receptor which is expressed in oviduct epithelium (Eil, 1992; Maclean et al., 2020; Pelletier et al., 2000). In testes epithelium, loss of the androgen receptor has shown to impair functional tight junction formation (Gye & Ohsako, 2003; Wang et al., 2006). There is a lot of circumstantial literature supporting these hypotheses. To elucidate the mechanism whether there is translocation of the cell-cell contact zone, the cell-cell junctions are affected, or there is a change in cytoskeleton due to DES and KTZ exposure, transcriptomic and proteomic analysis should be performed to provide insight on a molecular level.

Although the overall degree of ciliation in the BOEC-ALI system was low, there was an unexpected statistically significant decrease in the degree of secondary cilia observed after 10^{-9} M and 10^{-5} M DES exposure. Some data suggest that estrogenic exposure may have a stimulating effect in OEC ciliation. For example, an *in vivo* study showed increased differentiation and ciliation of oviduct epithelial cells after intramuscular injection of estrogen or DES in the chick (Anderson & Hein, 1976). Moreover, as previously mentioned, there is increased ciliation of the bovine oviduct epithelium during the follicular phase of the estrous cycle when E2 is high (Abe & Oikawa, 1993; Yániz et al., 2000). Additionally, DES exposed oocytes showed increased stabilization of microtubules, a key component of cilium formation (Ding et al., 2020). One explanation is that the loss of apical position of cell-cell adherence between BOECs is a result of alterations in tight junctions at the contact zone, causing the contact zone to dynamically move to a more basal position at the lateral side of two adjacent BOECs. This phenomenon could be a result of, or followed by, loss of BOEC polarity and therefore cause the decrease of cilia. Tight junctions are

known to maintain the apical-basal polarity of epithelial cells and subsequently polarity is essential for cilia formation and ciliary beating (Nakayama et al., 2021; Otani et al., 2019; Shin et al., 2006; Zihni et al., 2016).

To determine whether the lowered position of lateral cell-cell adherence as well as the decrease in secondary cilia observed after DES exposure was reversible, DES exposed monolayers were allowed to recover by culturing them for four days without DES. Monolayers exposed to 10^{-9} M DES showed, after a recovery period, approximately the same extent of lowered lateral position of cell-cell adherence as directly after exposure. Interestingly, monolayers exposed to 10^{-5} M DES showed a decrease in the extent of the lowered position of lateral cell-cell adherence, but to a lesser extent compared to recovered monolayers after 10^{-7} M DES exposure. Interestingly, TEER values of monolayers recovered from 10^{-9} M and 10^{-7} M DES exposure increased, whereas this increase was lesser for monolayers recovered from 10^{-5} M DES exposure. This is contradictory to the negative correlation observed between TEER values and the lowered position of lateral cell-cell adherence directly after DES exposure. If DES causes an effect on a proteomic level, recovery of four-days was expected to be sufficient. Moreover, studies have reported that DES exposure can alter epigenetic patterns (Bromer et al., 2009; Crews & McLachlan, 2006; Li et al., 2003). Epigenetic changes are potentially reversible, however, the temporal relation difficult to comprehend/estimate. Therefore, the lowered position of lateral cell-cell adherence is not necessarily caused by reversible mechanisms. It is noteworthy that only one replicate of this experiment was performed, and data should be confirmed by additional replicates.

Here, we showed that four-day culture of SOF in the apical compartment of Transwell® inserts does not affect BOEC monolayer confluency. More importantly, SOF incubation did not affect BOEC morphology and differentiation, confirmed by unaltered secondary ciliation rates, regardless of the SOF volume. Subsequently, we co-cultured presumably fertilized zygotes from *in vitro* embryo production (IVP) day 1-5 in the apical compartment of Transwell® inserts with a confluent BOEC monolayer. Unfortunately, day 5 cleavage rate was noticeably lower compared to conventional IVP and in total two day 8 blastocysts were produced in the BOEC-ALI co-culture system. Previously, two studies showed successful blastocyst formation in an BOEC-ALI co-culture culture, however, their experimental design differs from ours (Chen et al., 2017; Jordaens et al., 2020). Chen et al. (2017) established a 33-day BOEC-ALI culture, and co-culture was performed using 10-30 presumed zygotes per monolayer and reached day 8 blastocyst yield of 7%. Remarkably, the BOECs in culture produced and secreted approximately 20 µl oviductal fluid surrogate (OFS), which contained approximately 97% of the same proteins abundant in *in vivo* oviductal fluid. Further, oviductal glycoprotein 1 (OVGP1) was detected, the most abundant glycoprotein in oviductal fluid and important for the microenvironment supporting gamete maturation and fertilization (Chen et al., 2017; Zhao et al., 2022). In our model production and secretion of OVGP1 was not tested and SOF was not supplemented with OVGP1, however, the presence of OVGP1 could stimulate early embryonic development. In the second study, Jordaens et al. (2017) maintained a BOEC-ALI for 9 days before 20-35 presumed zygotes were co-cultured and a 14% day 8 blastocyst rate was acquired. For both studies, day 8 blastocyst yield is not as successful as conventional IVP, but it indicates the possibility of embryo co-culture in the BOEC-ALI system (Chen et al., 2017; Jordaens et al., 2020). Previously, we described the low percentage of secondary cilia in our BOEC-ALI culture, and possible ways to increase this percentage. In contrast, the importance of ciliation degree for embryo co-culture is unknown. After ovulation, E2 rapidly decreases while progesterone (P4) concentration rises. Bovine studies have shown that during the luteal phase, when P4 is high, the infundibulum and ampulla are predominated by secretory cells (Abe & Oikawa, 1993). This data suggests that during the early embryonic development, when E2 is low and P4 is increasing, the degree of ciliation of the OECs changes. Whether increasing ciliation rates of our BOEC-ALI culture will stimulate embryo co-culture and therefore day 8 blastocysts rates are something that should be elucidated. Possibly, optimization of our 23-day BOEC-ALI culture could increase BOEC functionality and subsequently their

supporting effect on early embryo development resulting in an increased blastocyst yield. Prior to using the BOEC-ALI embryo co-culture model for DES and KTZ testing, the establishment of a standardized and reproducible blastocyst production protocol and the quantification of DES and KTZ transference over the BOEC monolayer, if any, are necessary.

One limitation of the techniques used in the BOEC-ALI culture I want to emphasize here, is the sensitivity of the TEER measurement. The sensitivity of the technique to environmental factors (*e.g.* temperature changes (Blume et al., 2010) and media composition (Robilliard et al., 2018)) causes limited uniformity in literature and no universally accepted cut-off TEER value that characterises a good quality oviduct epithelium. For example, there is one suggested acceptable TEER range of 500-1100 $\Omega*cm^2$ (Chen et al., 2015), which was further used to validate TEER values in other studies (Jordaens et al., 2015; Leemans et al., 2022). However, our control monolayers displayed an average TEER of 1311 $\Omega*cm^2$, not within the range suggested by Chen et al. (2015). It should be noted, though, that TEER protocols followed differ in media composition. Chen et al. (2015) performed TEER in fetal bovine serum (FBS) supplemented media, contradictory to our FBS-free media. FBS is a factor that was recently shown to decrease TEER values with ~20% (Robilliard et al., 2018).This susceptibility of the TEER measurement makes comparisons with other literature and setting a cut-off value difficult.

In conclusion, we explored a bovine oviduct epithelial cell culture, to mimic the *in vivo* oviductal epithelium, as a model for EDC reproductive toxicity testing. We were able to establish BOEC monolayer cultures that recapitulate epithelial barrier function, but they were not able to support early embryo development. Diethylstilbestrol and ketoconazole exposure resulted in quantifiable effects (i.e., lateral cell-cell attachment) on the monolayers, suggesting the sensitivity of this model to EDC action. Functionality of the ALI culture needs to be optimized to better support BOEC ciliation and *in vivo*-like secretion. The model could then be used to study effects of indirect EDC exposure in co-cultured embryos. Eventually, the indirect exposure model should be compared to *in vivo* animal testing to validate the model.

Acknowledgements

I would like to thank the following people, without whom I would never have been able to conduct this research. I would like to thank my supervisors Nadia Asimaki and Bart Gadella for all the help, guidance, feedback, support, and much more. Moreover, I would like to thank Christine Oei for all the help with the oviduct culture, Hilde Aardema for the meetings, Pleun Jornick and Kaylee Nieuwland for the help in the lab and our brainstorm sessions, Esther van 't Veld for the introduction of the Nikon microscope, Richard Wubbolts who helped me with the NIS elements software.

References

Abe, H., & Hoshi, H. (1997). Bovine oviductal epithelial cells: Their cell culture and applications in studies for reproductive biology. *Cytotechnology*, *23*, 171–183. https://doi.org/10.1023/A:1007929826186

Abe, H., & Oikawa, T. (1993). Observations by scanning Electron Microscopy of Oviductal Epithelial Cells From Cows at Follicular and Luteal Phases. *Journal of Anatomy*, *235*, 399–410. https://doi.org/10.1002/ar.1092350309

Adam, A. H. B., de Haan, L. H. J., Estruch, I. M., Hooiveld, G. J. E. J., Louisse, J., & Rietjens, I. M. C. M. (2020). Estrogen receptor alpha (ERα)–mediated coregulator binding and gene expression discriminates the toxic ERα agonist diethylstilbestrol (DES) from the endogenous ERα agonist 17β-estradiol (E2). *Cell Biology and Toxicology*, *36*(5), 417–435. https://doi.org/10.1007/s10565-020-09516-6

Adedeji, O. B., Durhan, E. J., Garcia-Reyero, N., Kahl, M. D., Jensen, K. M., Lalone, C. A., Makynen, E. A., Perkins, E. J., Thomas, L., Villeneuve, D. L., & Ankley, G. T. (2012). Short-term study investigating the estrogenic potency of diethylstilbesterol in the fathead minnow (Pimephales promelas). *Environmental Science and Technology*, *46*(14), 7826–7835. https://doi.org/10.1021/es301043b

Alberts, B., Johnson, A., & Lewis, J. (2002). Fibroblasts and their transformations: the connective-tissue cell family. In *Molecular Biology of the Cell. 4th edition*.

Almiñana, C., Corbin, E., Tsikis, G., Alcântara-Neto, A. S., Labas, V., Reynaud, K., Galio, L., Uzbekov, R., Garanina, A. S., Druart, X., & Mermillod, P. (2017). Oviduct extracellular vesicles protein content and their role during oviduct–embryo cross-talk. *Reproduction*, *154*(3), 253–268. https://doi.org/10.1530/REP-17-0054

Alwis, I. D., Maroni, D. M., Hendry, I. R., Roy, S. K., May, J. V., Leavitt, W. W., & Hendry, W. J. (2011). Neonatal diethylstilbestrol exposure disrupts female reproductive tract structure/function via both direct and indirect mechanisms in the hamster. *Reproductive Toxicology*, *32*(4), 472–483. https://doi.org/10.1016/j.reprotox.2011.09.006

Amir, A. A., Kelly, J. M., Kleemann, D. O., Durmic, Z., Blache, D., & Martin, G. B. (2018). Phyto-oestrogens affect fertilisation and embryo development in vitro in sheep. *Reproduction, Fertility and Development*, *30*, 1109–1115. https://doi.org/10.1071/RD16481

Anderson, J. M. (2001). Molecular structure of tight junctions and their role in epithelial transport. *News in Physiological Sciences*, *16*(3), 126–130. https://doi.org/10.1152/physiologyonline.2001.16.3.126

Anderson, R. ., & Hein, C. . (1976). Estrogen dependent ciliogenesis in the chick oviduct. *Cell and Tissue Research*, *171*(4), 459–466. https://doi.org/10.1007/BF00220238

Asimaki, K., Vazakidou, P., van Tol, H. T. A., Oei, C. H. Y., Modder, E. A., van Duursen, M. B. M., & Gadella, B. M. (2022). Bovine In Vitro Oocyte Maturation and Embryo Production Used as a Model for Testing Endocrine Disrupting Chemicals Eliciting Female Reproductive Toxicity With Diethylstilbestrol as a Showcase Compound. *Frontiers in Toxicology*, *4*, 1–19. https://doi.org/10.3389/ftox.2022.811285

Baravalle, R., Ciaramella, A., Baj, F., Di Nardo, G., & Gilardi, G. (2018). Identification of endocrine disrupting chemicals acting on human aromatase. *Biochimica et Biophysica Acta - Proteins and Proteomics*, *1866*(1), 88–96. https://doi.org/10.1016/j.bbapap.2017.05.013

Bissell, M. J. (1981). The Differentiated State of Normal and Malignant Cells or How to Define a "Normal" Cell in Culture. In *International Review of Cytology* (Vol. 70). https://doi.org/10.1016/S0074-7696(08)61130-4

Blume, L. F., Denker, M., Gieseler, F., & Kunze, T. (2010). Temperature corrected transepithelial

electrical resistance (TEER) measurement to quantify rapid changes in paracellular permeability. *Pharmazie*, *65*(1), 19–24. https://doi.org/10.1691/ph.2010.9665

Bolger, R., Wiese, T. E., Ervin, K., Nestich, S., & Checovich, W. (1998). Rapid Screening of Environmental Chemicals for Estrogen Receptor Binding Capacity. *Environmental Health*, *106*(9), 551–557. https://doi.org/10.1289/ehp.98106551

Brevini, T. A. L., Cillo, F., Antonini, S., & Gandolfi, F. (2005). Effects of endocrine disrupters on the oocytes and embryos of farm animals. *Reproduction in Domestic Animals*, *40*(4), 291–299. https://doi.org/10.1111/j.1439-0531.2005.00592.x

Bromer, J. G., Wu, J., Zhou, Y., & Taylor, H. S. (2009). Hypermethylation of homeobox A10 by in utero diethylstilbestrol exposure: An epigenetic mechanism for altered developmental programming. *Endocrinology*, *150*(7), 3376–3382. https://doi.org/10.1210/en.2009-0071

Chen, S., Einspanier, R., & Schoen, J. (2013a). In vitro mimicking of estrous cycle stages in porcine oviduct epithelium cells: Estradiol and progesterone regulate differentiation, gene expression, and cellular function. *Biology of Reproduction*, *89*(3), 1–12. https://doi.org/10.1095/biolreprod.113.108829

Chen, S., Einspanier, R., & Schoen, J. (2013b). Long-term culture of primary porcine oviduct epithelial cells: Validation of a comprehensive invitro model for reproductive science. *Theriogenology*, *80*(8), 862–869. https://doi.org/10.1016/j.theriogenology.2013.07.011

Chen, S., Einspanier, R., & Schoen, J. (2015). Transepithelial electrical resistance (TEER): a functional parameter to monitor the quality of oviduct epithelial cells cultured on filter supports. *Histochemistry and Cell Biology*, *144*(5), 509–515. https://doi.org/10.1007/s00418-015-1351-1

Chen, S., Palma-Vera, S. E., Langhammer, M., Galuska, S. P., Braun, B. C., Krause, E., Lucas-Hahn, A., & Schoen, J. (2017). An air-liquid interphase approach for modeling the early embryo-maternal contact zone. *Scientific Reports*, *7*, 1–7. https://doi.org/10.1038/srep42298

Chen, S., & Schoen, J. (2021). Using the Air–Liquid Interface Approach to Foster Apical–Basal Polarization of Mammalian Female Reproductive Tract Epithelia In Vitro. *Methods in Molecular Biology*, *2273*, 251–262. https://doi.org/10.1007/978-1-0716-1246-0_18

Crews, D., & McLachlan, J. A. (2006). Epigenetics, evolution, endocrine disruption, health, and disease. *Endocrinology*, *147*(6). https://doi.org/10.1210/en.2005-1122

Delbes, G., Blázquez, M., Fernandino, J. I., Grigorova, P., Hales, B. F., Metcalfe, C., Navarro-Martín, L., Parent, L., Robaire, B., Rwigemera, A., Van Der Kraak, G., Wade, M., & Marlatt, V. (2022). Effects of endocrine disrupting chemicals on gonad development: Mechanistic insights from fish and mammals. *Environmental Research*, *204*. https://doi.org/10.1016/j.envres.2021.112040

Ding, Z. M., Hua, L. P., Ahmad, M. J., Safdar, M., Chen, F., Wang, Y. S., Zhang, S. X., Miao, Y. L., Xiong, J. J., & Huo, L. J. (2020). Diethylstilbestrol exposure disrupts mouse oocyte meiotic maturation in vitro through affecting spindle assembly and chromosome alignment. *Chemosphere*, *249*, 126182. https://doi.org/10.1016/j.chemosphere.2020.126182

Dodds, E. ., Goldberg, L., Lawson, W., & Robinson, R. (1938). Estrogenic activity of certain synthetic compounds. *Nature*, *3562*, 247–248. https://doi.org/10.1038/141247b0

Eil, C. (1992). Ketoconazole binds to the human androgen receptor. *Hormone and Metabolic Research*, *24*(8), 367–370. https://doi.org/10.1055/s-2007-1003337

Ferraz, M. A. M. M., Henning, H. H. W., Stout, T. A. E., Vos, P. L. A. M., & Gadella, B. M. (2017). Designing 3-Dimensional In Vitro Oviduct Culture Systems to Study Mammalian Fertilization and Embryo Production. *Annals of Biomedical Engineering*, *45*(7), 1731–1744. https://doi.org/10.1007/s10439-016-1760-x

Ferraz, M. A. M. M., Rho, H. S., Hemerich, D., Henning, H. H. W., van Tol, H. T. A., Hölker, M., Besenfelder, U., Mokry, M., Vos, P. L. A. M., Stout, T. A. E., Le Gac, S., & Gadella, B. M. (2018). An oviduct-on-a-chip provides an enhanced in vitro environment for zygote genome reprogramming. *Nature Communications*, *9*(1). https://doi.org/10.1038/s41467-018-07119-8

Galli, C., Duchi, R., Crotti, G., Turini, P., Ponderato, N., Colleoni, S., Lagutina, I., & Lazzari, G. (2003). Bovine embryo technologies. *Theriogenology*, *59*(2), 599–616. https://doi.org/10.1016/S0093-691X(02)01243-8

Gandolfi, F., & Moor, R. M. (1987). Stimulation of early embryonic development in the by co-culture with oviduct epithelial cells. *Journal of Reproduction and Fertility*, *81*(1), 23–28. https://doi.org/10.1530/jrf.0.0810023

Gardiner, C. S., Menino, A. R., Archibong, A. E., Williams, J. S., Stormshak, F., & England, D. C. (1988). Suppressed development of cultured mouse and swine embryos by diethylstilbestrol. *Journal of Animal Science*, *66*, 2401–2406. https://doi.org/10.2527/jas1988.6692401x

Giusti, R. M., Iwamoto, K., & Hatch, E. E. (1995). Diethylstilbestrol revisited: A review of the long-term health effects. *Annals of Internal Medicine*, *122*(10), 778–788. https://doi.org/10.7326/0003-4819-122-10-199505150-00008

González-Brusi, L., Algarra, B., Moros-Nicolás, C., Izquierdo-Rico, M. J., Avilés, M., & Jiménez-Movilla, M. (2020). A comparative view on the oviductal environment during the periconception period. *Biomolecules*, *10*(12), 1–25. https://doi.org/10.3390/biom10121690

Gorodeski, G. I. (2007). Estrogen decrease in tight junctional resistance involves matrix-metalloproteinase-7-mediated remodeling of occludin. *Endocrinology*, *148*(1), 218–231. https://doi.org/10.1210/en.2006-1120

Gorodeski, G. I., & Pal, D. (2000). Involvement of estrogen receptors α and β in the regulation of cervical permeability. *American Journal of Physiology - Cell Physiology*, *278*, 689–696. https://doi.org/10.1152/ajpcell.2000.278.4.c689

Gualtieri, R., Mollo, V., Braun, S., Barbato, V., Fiorentino, I., & Talevi, R. (2012). Long-term viability and differentiation of bovine oviductal monolayers: Bidimensional versus three-dimensional culture. *Theriogenology*, *78*(7), 1456–1464. https://doi.org/10.1016/j.theriogenology.2012.06.010

Gye, M., & Ohsako, S. (2003). Effects of flutamide in the rat testis on the expression of occludin, an integral member of tight junctions. *Toxicology Letters*, *143*(2), 217–222. https://doi.org/10.1016/S0378-4274(03)00178-4

Herbst, A. L., Ulfelder, H., & Poskanzer, D. C. (1971). Adenocarcinoma of the Vigina - Association of Maternal Stilbestrol Therapy with Tumor Appearance in Young Women. *New England Journal of Medicine*, *284*(16), 878–881. https://doi.org/10.1056/NEJM197104222841604

Hoelzle, M. K., & Svitkina, T. (2012). The cytoskeletal mechanisms of cell-cell junction formation in endothelial cells. *Molecular Biology of the Cell*, *23*(2), 310–323. https://doi.org/10.1091/mbc.E11-08-0719

Inman, J. L., & Bissell, M. J. (2010). Apical polarity in three-dimensional culture systems: Where to now? *Journal of Biology*, *9*(2). https://doi.org/10.1186/jbiol213

International Programme on Chemical Safety. (2002). *Global assessment on the state of the science of endocrine disruptors*. https://apps.who.int/iris/handle/10665/67357

Ireland, J. J., Murphee, R. L., & Coulson, P. B. (1980). Accuracy of Predicting Stages of Bovine Estrous Cycle by Gross Appearance of the Corpus Luteum. *Journal of Dairy Science*, *63*(1), 155–160. https://doi.org/10.3168/jds.S0022-0302(80)82901-8

Janevski, J., Choh, V., Stopper, H., Schiffmann, D., & De Boni, U. (1993). Diethylstilbestrol alters the morphology and calcium levels of growth cones of PC12 cells in vitro. *Neurotoxicity*, *14*(4), 505–511.

Jordaens, L., Arias-Alvarez, M., Pintelon, I., Thys, S., Valckx, S., Dezhkam, Y., Bols, P. E. J., & Leroy, J. L. M. R. (2015). Elevated non-esterified fatty acid concentrations hamper bovine oviductal epithelial cell physiology in three different in vitro culture systems. *Theriogenology*, *84*, 899–910. https://doi.org/10.1016/j.theriogenology.2015.05.030

Jordaens, L., Van Hoeck, V., Pintelon, I., Thys, S., Bols, P. E. J., Marei, W. F. A., & Leroy, J. L. M. R. (2020). Altered embryotrophic capacities of the bovine oviduct under elevated free fatty acid conditions: An in vitro embryo-oviduct co-culture model. *Reproduction, Fertility and Development*, *32*(6), 553–563. https://doi.org/10.1071/RD19019

King, C. T., Rogers, P. D., Cleary, J. D., & Chapman, S. W. (1998). Antifungal therapy during pregnancy. *Clinical Infectious Diseases*, *27*(5), 1151–1160. https://doi.org/10.1086/514977

Kjærstad, M. B., Taxvig, C., Nellemann, C., Vinggaard, A. M., & Andersen, H. R. (2010). Endocrine disrupting effects in vitro of conazole antifungals used as pesticides and pharmaceuticals. *Reproductive Toxicology*, *30*(4), 573–582. https://doi.org/10.1016/j.reprotox.2010.07.009

Kress, A., & Morson, G. (2007). Changes in the oviducal epithelium during the estrous cycle in the marsupial Monodelphis domestica. *Journal of Anatomy*, *211*(4), 503–517. https://doi.org/10.1111/j.1469-7580.2007.00794.x

Leemans, B., Bromfield, E. G., Stout, T. A. E., Vos, M., Van Der Ham, H., Van Beek, R., Van Soom, A., Gadella, B. M., & Henning, H. (2022). Developing a reproducible protocol for culturing functional confluent monolayers of differentiated equine oviduct epithelial cells. *Biology of Reproduction*, *106*(4), 710–729. https://doi.org/10.1093/biolre/ioab243

Leese, H. J., Tay, J. I., Reischl, J., & Downing, S. J. (2001). Formation of Fallopian tubal fluid: role of a neglected epithelium. *Reproduction*, *121*(3), 339–346. https://doi.org/10.1530/rep.0.1210339

Li, S., Hansman, R., Newbold, R., Davis, B., McLachlan, J. A., & Barrett, J. C. (2003). Neonatal diethylstilbestrol exposure induces persistent elevation of c-fos expression and hypomethylation in its Exon-4 in mouse uterus. *Molecular Carcinogenesis*, *38*(2), 78–84. https://doi.org/10.1002/mc.10147

Loose, D. S., Kan, P. B., Hirst, M. A., Marcus, R. A., & Feldman, D. (1983). Ketoconazole Blocks Adrenal Steroidogenesis by Inhibiting Cytochrome P450-dependent Enzymes. *The Journal of Clinical Investigation*, *71*(5), 1495–1499. https://doi.org/10.1172/JCI110903

Lopera Vasquez, R., Uribe-García, F., & Rondón-Barragán, I. (2022). Effect of Estrous Cycle Phases on Gene Expression of Bovine Oviduct Epithelial Cells. *Vetinary World*, *15*. https://doi.org/10.2139/ssrn.3949261

Lyons, R. A., Djahanbakhch, O., Mahmood, T., Saridogan, E., Sattar, S., Sheaff, M. T., Naftalin, A. A., & Chenoy, R. (2002). Fallopian tube ciliary beat frequency in relation to the stage of menstrual cycle and anatomical site. *Human Reproduction*, *17*(3), 584–588. https://doi.org/10.1093/humrep/17.3.584

Ma, Y., He, X., Qi, K., Wang, T., Qi, Y., Cui, L., Wang, F., & Song, M. (2019). Effects of environmental contaminants on fertility and reproductive health. *Journal of Environmental Sciences*, *77*, 210–217. https://doi.org/10.1016/J.JES.2018.07.015

Maclean, A., Bunni, E., Makrydima, S., Withington, A., Kamal, A. M., Valentijn, A. J., & Hapangama, D. K. (2020). Fallopian tube epithelial cells express androgen receptor and have a distinct hormonal responsiveness when compared with endometrial epithelium. *Human Reproduction*, *35*(9), 2097–2106. https://doi.org/10.1093/humrep/deaa177

Maillo, V., Gaora, P., Forde, N., Besenfelder, U., Havlicek, V., Burns, G. W., Spencer, T. E., Gutierrez-Adan, A., Lonergan, P., & Rizos, D. (2015). Oviduct-embryo interactions in cattle: Two-way traffic or a one-way street? *Biology of Reproduction*, *92*(6), 1–8. https://doi.org/10.1095/biolreprod.115.127969

Ménézo, Y. J. R., & Hérubel, F. (2002). Mouse and bovine models for human IVF. *Reproductive Biomedicine Online*, *4*(2), 170–175. https://doi.org/10.1016/S1472-6483(10)61936-0

Mikamo, H., Kawazoe, K., Sato, Y., Izumi, K., Ito, T., Ito, K., & Tamaya, T. (1999). Penetration of oral fluconazole into gynecological tissues. *Antimicrobial Agents and Chemotherapy*, *43*(1), 148–151. https://doi.org/10.1128/aac.43.1.148

Munkboel, C. H., Rasmussen, T. B., Elgaard, C., Olesen, M. L. K., Kretschmann, A. C., & Styrishave, B. (2019a). The classic azole antifungal drugs are highly potent endocrine disruptors in vitro inhibiting steroidogenic CYP enzymes at concentrations lower than therapeutic Cmax. *Toxicology*, *425*(July), 152247. https://doi.org/10.1016/j.tox.2019.152247

Munkboel, C. H., Rasmussen, T. B., Elgaard, C., Olesen, M. L. K., Kretschmann, A. C., & Styrishave, B. (2019b). The classic azole antifungal drugs are highly potent endocrine disruptors in vitro inhibiting steroidogenic CYP enzymes at concentrations lower than therapeutic Cmax. *Toxicology*, *425*, 152247. https://doi.org/10.1016/j.tox.2019.152247

Nadal, A., Ropero, A. B., Laribi, O., Maillet, M., Fuentes, E., & Soria, B. (2000). Nongenomic actions of estrogens and xenoestrogens by binding at a plasma membrane receptor unrelated to estrogen receptor α and estrogen receptor β. *Proceedings of the National Academy of Sciences of the United States of America*, *97*(21), 11603–11608. https://doi.org/10.1073/pnas.97.21.11603

Nakayama, S., Yano, T., Namba, T., Konishi, S., Takagishi, M., Herawati, E., Nishida, T., Imoto, Y., Ishihara, S., Takahashi, M., Furuta, K., Oiwa, K., Tamura, A., & Tsukita, S. (2021). Planar cell polarity induces local microtubule bundling for coordinated ciliary beating. *Journal of Cell Biology*, *220*(7). https://doi.org/10.1083/jcb.202010034

Newbold, R. R., Bullock, B. C., & Mc Lachlan, J. A. (1983). Exposure to diethylstilbestrol during pregnancy permanently alters the ovary and oviduct. *Biology of Reproduction*, *28*(3), 735–744. https://doi.org/10.1095/biolreprod28.3.735

Otani, T., Nguyen, T. P., Tokuda, S., Sugihara, K., Sugawara, T., Furuse, K., Miura, T., Ebnet, K., & Furuse, M. (2019). Claudins and JAM-A coordinately regulate tight junction formation and epithelial polarity. *Journal of Cell Biology*, *218*(10), 3372–3396. https://doi.org/10.1083/JCB.201812157

Pelletier, C., Labrie, C., & Labrie, F. (2000). Localization of oestrogen receptor α, oestrogen receptor β and androgen receptors in the rat reproductive organs. *Journal of Endocrinology*, *165*(2), 359–370. https://doi.org/10.1677/joe.0.1650359

Pérez-Cerezales, S., Ramos-Ibeas, P., Acuna, O. S., Avilés, M., Coy, P., Rizos, D., & Gutieŕrez-Adán, A. (2018). The oviduct: From sperm selection to the epigenetic landscape of the embryo. *Biology of Reproduction*, *98*(3), 262–276. https://doi.org/10.1093/biolre/iox173

Qiu, X., Li, X., Wu, Z., Zhang, F., Wang, N., Wu, N., Yang, X., & Liu, Y. (2016). Fungal-bacterial interactions in mice with dextran sulfate sodium (DSS)-induced acute and chronic colitis. *RSC Advances*, *6*(70), 65995–66006. https://doi.org/10.1039/c6ra03869g

Rajagopal, M., Tollner, T. L., Finkbeiner, W. E., Cherr, G. N., & Widdicombe, J. H. (2006). Differentiated structure and function of primary cultures of monkey oviductal epithelium. *In Vitro Cellular and Developmental Biology - Animal*, *42*, 248–254. https://doi.org/10.1290/0602015

Reischl, J., Prelle, K., Schöl, H., Neumüller, C., Einspanier, R., Sinowatz, F., & Wolf, E. (1999). Factors affecting proliferation and dedifferentiation of primary bovine oviduct epithelial cells in

vitro. *Cell and Tissue Research*, *296*, 371–383. https://doi.org/10.1007/s004410051297

Rizos, D., Maillo, V., Sánchez-Calabuig, M. J., & Lonergan, P. (2017). The Consequences of maternal-embryonic cross talk during the periconception period on subsequent embryonic development. In *Periconception in Physiology and Medicine* (Vol. 1014, pp. 69–86). https://doi.org/10.1007/978-3-319-62414-3_4

Robilliard, L. D., Kho, D. T., Johnson, R. H., Anchan, A., O'Carroll, S. J., & Graham, E. S. (2018). The importance of multifrequency impedance sensing of endothelial barrier formation using ECIS technology for the generation of a strong and durable paracellular barrier. *Biosensors*, *8*(3). https://doi.org/10.3390/bios8030064

Rothschild, T. ., Calhoon, R. ., & Boylan, E. . (1987). Genital tract abnormalities in female rats exposed to diethylstilbestrol in utero. *Reproductive Toxicology*, *1*(3), 193–202. https://doi.org/10.1016/S0890-6238(87)80033-3

Rottmayer, R., Ulbrich, S. E., Kölle, S., Prelle, K., Neumueller, C., Sinowatz, F., Meyer, H. H. D., Wolf, E., & Hiendleder, S. (2006). A bovine oviduct epithelial cell suspension culture system suitable for studying embryo-maternal interactions: Morphological and functional characterization. *Reproduction*, *132*(4), 637–648. https://doi.org/10.1530/rep.1.01136

Santos, R. ., Schoevers, E. ., & Roelen, B. A. . (2014). Usefulness of bovine and porcine IVM/IVF models for reproductive toxicology. *Reproductive Biology and Endocrinology*, *12*(117). http://www.embase.com/search/results?subaction=viewrecord&from=export&id=L603249436%0Ahttp://dx.doi.org/10.1186/1477-7827-12-117

Senger, P. . (1997). The luteal phase of the estrous cycle. In *Pathways to pregnancy and parturition. 1st revised edition* (p. 152).

Seo, H.-W., Park, K.-J., Lee, H.-C., Kim, D.-Y., Song, Y.-S., Lim, J.-M., Song, G.-H., & Han, J.-Y. (2009). Physiological Effects of Diethylstilbestrol Exposure on the Development of the Chicken Oviduct. *Journal of Animal Science and Technology*, *51*(6), 485–492. https://doi.org/10.5187/jast.2009.51.6.485

Shin, K., Fogg, V. C., & Margolis, B. (2006). Tight junctions and cell polarity. *Annual Review of Cell and Developmental Biology*, *22*, 207–235. https://doi.org/10.1146/annurev.cellbio.22.010305.104219

Sonino, N. (1987). The use of Ketoconazole as an Inhibitor of Steroid Production. *New England Journal of Medicine*, *317*(13), 812–818. https://doi.org/10.1056/NEJM198709243171307

Srinivasan, B., Kolli, A. ., Esch, M. ., Abaci, H. ., Shuler, L., & Hickman, J. J. (2015). TEER measurement techniques for in vitro barrier model systems. In *Journal of Laboratory Automation* (Vol. 20, Issue 2). https://doi.org/10.1177/2211068214561025.TEER

Thibodeaux, J. ., & Godke, R. . (1992). In vitro enhancement of early-stage embryos with co-culture. *Archives of Pathology & Laboratory Medicine*, *116*(4), 364–372.

Tsafriri, A., Popliker, M., Nahum, R., & Beyth, Y. (1998). Effects of ketoconazole on ovulatory changes in the rat: Implications on the role of a meiosis-activating sterol. *Molecular Human Reproduction*, *4*(5), 483–489. https://doi.org/10.1093/molehr/4.5.483

Ulbrich, S. E., Zitta, K., Hiendleder, S., & Wolf, E. (2010). In vitro systems for intercepting early embryo-maternal cross-talk in the bovine oviduct. *Theriogenology*, *73*(6), 802–816. https://doi.org/10.1016/j.theriogenology.2009.09.036

Walker, S. K., Hartwich, K. M., & Robinson, J. S. (2000). Long-term effects on offspring of exposure of oocytes and embryos to chemical and physical agents. *Human Reproduction Update*, *6*(6), 564–577. https://doi.org/10.1093/humupd/6.6.564

Wang, R. S., Yeh, S., Chen, L. M., Lin, H. Y., Zhang, C., Ni, J., Wu, C. C., Di Sant'Agnese, P. A., DeMesy-Bentley, K. L., Tzeng, C. R., & Chang, C. (2006). Androgen receptor in Sertoli cell is essential

for germ cell nursery and junctional complex formation in mouse testes. *Endocrinology*, *147*(12), 5624–5633. https://doi.org/10.1210/en.2006-0138

Yániz, J. ., Lopez-Catios, F., Santolaria, P., & Mullins, K. . (2000). Study of the Functional Anatomy of Bovine Oviductal Mucosa. *Scanning Electron Microscopy*, *260*, 268–278. https://doi.org/10.1002/1097-0185(20001101)260:3<268::AID-AR60>3.0.CO;2-L.

Zarn, J. A., Brüschweiler, B. J., & Schlatter, J. R. (2003). Azole fungicides affect mammalian steroidogenesis by inhibiting sterol 14α-demethylase and aromatase. *Environmental Health Perspectives*, *111*(3), 255–261. https://doi.org/10.1289/ehp.5785

Zeng, R., Li, X., & Gorodeski, G. I. (2004). Estrogen abrogates transcervical tight junctional resistance by acceleration of occludin modulation. *Journal of Clinical Endocrinology and Metabolism*, *89*(10), 5145–5155. https://doi.org/10.1210/jc.2004-0823

Zhao, Y., Vanderkooi, S., & Kan, F. W. K. (2022). The role of oviduct-specific glycoprotein (OVGP1) in modulating biological functions of gametes and embryos. *Histochemistry and Cell Biology*, *157*, 371–388. https://doi.org/10.1007/s00418-021-02065-x

Zhu, L., Li, X., Zeng, R., & Gorodeski, G. I. (2006). Changes in tight junctional resistance of the cervical epithelium are associated with modulation of content and phosphorylation of occludin 65-kilodalton and 50-kilodalton forms. *Endocrinology*, *147*(2), 977–989. https://doi.org/10.1210/en.2005-0916

Zihni, C., Mills, C., Matter, K., & Balda, M. S. (2016). Tight junctions: From simple barriers to multifunctional molecular gates. *Nature Reviews Molecular Cell Biology*, *17*(9), 564–580. https://doi.org/10.1038/nrm.2016.80

Supplementary data

Supplemental table 1: overview of number of replicates and total monolayers used for each experiment.

section	Experiment	replicate	group	total monolayers
I	Duration of BOEC-ALI culture	1	12 days	2
			15 days	2
			23 days	2
			6 weeks	6
	Pooled vs. non-pooled material	1	non pooled animal 1	6
			non pooled animal 2	6
			non pooled animal 3	6
			pooled	6
II	BOEC viability after EDC exposure	1	0,01% v/v DMSO	2
			10^{-9} M DES	2
			10^{-7} M DES	2
			10^{-5} M DES	2
			10^{-8} M KTZ	2
			10^{-7} M KTZ	2
			10^{-6} M KTZ	2
	Effect EDC exposure on BOEC monolayers (confluency, differentiation and morphology)	3	control	12
			0,01% v/v DMSO	6
			10^{-9} M DES	8
			10^{-7} M DES	8
			10^{-5} M DES	8
			10^{-8} M KTZ	6
			10^{-7} M KTZ	6
			10^{-6} M KTZ	6
	Recovery after DES exposure	1	10^{-9} M DES	2
			10^{-7} M DES	2
			10^{-5} M DES	2
III	Effect apical SOF incubation	2	50 µl SOF	2
			100 µl SOF	2
			150 µl SOF	2
	Embryo co-culture	1	6 zygotes 100 µl SOF	2
			6 zygotes 150 µl SOF	2
			15 zygotes 100 µl SOF	2
			15 zygotes 150 µl SOF	2
			30 zygotes 100 µl SOF	2
			30 zygotes 150 µl SOF	2

Supplemental table 2: All transepithelial electrical resistance (TEER) and paracellular tracer flux values corresponding to individual monolayers (n). DES 10^{-9} ^ is outlier.

			TEER Ω*cm²			Tracer flux %		
Condition	**Replicate**	***n***	**Before**	**after**	**change**	**Before**	**after**	**change**
Control	1	4	671	1158	487	0,10%	0,08%	-0,02%
			503	539	37	0,19%	0,28%	0,09%
			534	624	90	0,10%	0,55%	0,45%
			874	843	-31	0,11%	0,29%	0,18%
	2	4	1698	1513	-185	0,12%	0,11%	-0,01%
			1770	1494	-275	0,11%	0,13%	0,02%
			2025	2576	551	0,09%	0,10%	0,01%
			2028	1528	-499	0,08%	0,09%	0,01%
	3	4	1591	688	-903	0,16%	0,17%	0,02%
			1300	802	-498	0,81%	0,08%	-0,73%
			1138	719	-419	0,33%	0,07%	-0,26%
			1585	912	-672	0,09%	0,16%	0,06%
0.01 % v/v DMSO	1	2	580	609	28	0,09%	0,19%	0,10%
			673	398	-276	0,14%	0,23%	0,09%
	2	2	2020	2140	120	0,09%	0,27%	0,18%
			2018	1917	-101	0,05%	0,09%	0,03%
	3	2	1508	1308	-200	0,77%	0,07%	-0,70%
			1154	815	-339	1,58%	0,11%	-1,47%
10^{-9} M DES	1	2	669	347	-322	0,09%	0,10%	0,01%
			733^	2047^	1313^	0,11%	0,16%	0,05%
	2	4	1846	797	-1049	0,58%	0,12%	-0,45%
			1974	899	-1075	0,20%	0,24%	0,05%
			1973	520	-1453	0,11%	0,28%	0,17%
			1655	808	-847	0,09%	0,21%	0,12%
	3	2	1110	252	-858	0,08%	0,20%	0,12%
			811	295	-516	0,09%	0,21%	0,12%
10^{-7} M DES	1	2	619	225	-394	0,11%	0,52%	0,41%
			1055	335	-721	0,06%	0,25%	0,19%
	2	4	1860	862	-999	0,68%	0,15%	-0,53%
			1674	757	-917	0,15%	0,14%	0,00%
			2026	453	-1573	0,30%	0,22%	-0,07%
			1898	514	-1384	0,07%	0,14%	0,08%
	3	2	1020	318	-702	0,09%	0,20%	0,11%
			740	316	-424	0,09%	0,17%	0,08%
10^{-5} M DES	1	2	971	403	-568	0,06%	1,52%	1,46%
			1225	408	-817	0,05%	0,19%	0,13%
	2	4	1844	528	-1316	0,05%	0,36%	0,31%
			1570	404	-1166	0,06%	0,29%	0,23%
			1573	435	-1138	0,36%	0,20%	-0,16%
			2301	751	-1551	0,06%	0,19%	0,13%
	3	2	1200	217	-983	0,08%	0,19%	0,11%
			715	295	-420	0,09%	0,17%	0,08%
10^{-8} M KTZ	1	2	579	353	-227	0,10%	0,69%	0,60%
			543	419	-124	0,09%	0,43%	0,34%
	2	2	2513	957	-1556	0,10%	0,10%	0,00%
			1742	1052	-691	0,49%	0,17%	-0,33%
	3	2	1114	411	-703	0,08%	0,50%	0,42%
			1033	483	-550	0,08%	0,15%	0,07%
10^{-7} M KTZ	1	2	859	231	-628	0,08%	1,20%	1,13%
			565	312	-253	0,10%	0,17%	0,06%
	2	2	1987	1003	-984	0,06%	0,21%	0,15%
			1981	1444	-538	0,23%	0,09%	-0,14%
	3	2	1105	462	-643	0,10%	0,22%	0,13%
			928	359	-570	0,09%	0,30%	0,20%
10^{-6} M KTZ	1	2	690	464	-226	0,10%	0,13%	0,02%
			531	294	-237	0,13%	0,35%	0,22%
	2	2	1925	835	-1091	0,06%	0,17%	0,11%
			2041	942	-1098	0,07%	0,11%	0,04%
	3	2	1037	309	-728	0,07%	0,22%	0,16%
			725	262	-463	0,11%	0,16%	0,05%

Supplemental table 3: All secondary cilia percentages and categorization of lowered position of lateral cell-cell data corresponding to individual monolayers (n). For each monolayer 5 images were analysed (1-5).

			Secondary Cilia %					Lateral cell-cell adherence category				
Condition	**Replicate**	***n***	**1**	**2**	**3**	**4**	**5**	**1**	**2**	**3**	**4**	**5**
Control	1	4	0,00%	0,11%	0,00%	0,00%	0,26%	0	0	0	0	1
			0,14%	0,00%	0,64%	0,00%	0,00%	1	0	0	0	0
			3,62%	1,52%	0,00%	0,28%	0,30%	0	0	0	0	0
			0,00%	0,00%	1,20%	0,00%	0,00%	0	0	0	1	0
	2	4	0,00%	0,69%	1,67%	1,31%	0,00%	0	0	0	0	1
			0,00%	1,37%	0,00%	0,00%	0,43%	1	1	0	0	2
			0,00%	0,00%	6,78%	5,31%	1,12%	1	0	0	0	0
			0,26%	0,23%	0,00%	3,74%	0,00%	0	1	1	0	1
	3	4	0,00%	1,06%	x	x	x	0	0	x	x	x
			0,37%	1,00%	0,86%	0,99%	0,00%	0	0	0	0	0
			0,19%	0,00%	1,10%	0,14%	0,98%	0	0	0	0	0
			2,64%	1,52%	4,85%	0,00%	1,00%	0	0	0	0	0
0.01% v/v DMSO	1	2	0,00%	0,24%	0,39%	0,00%	3,59%	2	1	0	2	0
			0,00%	x	x	x	x	0	x	x	x	x
	2	2	0,00%	0,29%	0,00%	0,25%	0,62%	1	0	0	0	0
			0,00%	0,52%	1,16%	0,00%	0,00%	0	0	0	0	0
	3	2	0,50%	0,27%	8,43%	4,14%	1,04%	0	1	0	0	0
			11,65%	4,87%	1,44%	8,79%	9,94%	0	0	0	0	0
10^{-9} M DES	1	2	0,00%	0,00%	0,00%	0,00%	0,00%	4	3	0	1	0
			0,00%	0,00%	0,00%	0,00%	0,00%	4	2	4	4	4
	2	2	0,22%	1,15%	0,28%	0,00%	0,00%	4	1	3	3	1
			0,00%	0,00%	0,00%	0,00%	0,00%	3	2	3	1	2
	3	2	0,00%	0,00%	0,00%	0,00%	0,23%	2	3	1	3	3
			0,00%	0,00%	0,25%	0,00%	0,00%	3	3	0	2	4
10^{-7} M DES	1	2	0,00%	0,00%	0,00%	0,00%	0,00%	4	4	4	4	4
			0,00%	0,00%	0,00%	0,00%	0,00%	3	0	3	2	4
	2	2	0,00%	0,00%	0,00%	1,36%	0,14%	3	3	4	1	2
			0,00%	0,00%	0,00%	2,92%	0,00%	2	2	2	1	2
	3	4	0,34%	0,00%	0,00%	0,00%	0,19%	2	3	4	2	2
			0,00%	0,00%	0,00%	0,00%	0,00%	2	0	3	0	3
10^{-5} M DES	1	2	0,00%	0,00%	0,79%	0,19%	0,13%	3	0	0	1	1
			0,00%	0,00%	0,00%	0,00%	0,00%	4	2	3	0	1
	2	2	1,36%	1,80%	0,13%	0,00%	0,43%	1	1	4	2	0
			1,20%	0,12%	0,00%	2,37%	0,00%	0	3	3	1	4
	3	2	0,00%	0,00%	0,00%	0,00%	0,00%	0	2	2	4	4
			0,00%	0,00%	0,00%	0,08%	0,00%	2	3	2	2	3
10^{-8} M KTZ	1	2	0,00%	0,00%	0,15%	0,00%	0,00%	4	4	0	4	3
			x	x	x	x	x	x	x	x	x	x
	2	2	0,00%	0,00%	0,14%	0,00%	0,00%	2	3	3	2	2
			0,00%	0,21%	0,44%	0,00%	0,00%	4	4	3	1	3
	3	2	0,43%	0,00%	0,15%	0,00%	2,80%	2	2	1	3	1
			0,00%	0,00%	0,00%	0,00%	0,24%	2	3	2	3	0
10^{-7} M KTZ	1	2	0,00%	0,00%	0,20%	0,16%	0,00%	4	4	4	0	4
			0,00%	0,00%	0,00%	0,00%	0,00%	4	4	2	4	3
	2	2	2,97%	0,41%	0,97%	0,91%	0,00%	0	2	1	2	4
			1,84%	0,34%	0,00%	0,97%	0,22%	1	3	2	2	0
	3	2	0,00%	0,13%	0,00%	0,00%	0,00%	3	3	1	3	1
			0,00%	0,00%	0,00%	0,00%	0,00%	4	2	1	3	0
10^{-6} M KTZ	1	2	0,00%	0,00%	0,14%	0,00%	0,00%	4	3	0	3	3
			0,00%	0,00%	0,00%	0,00%	0,00%	3	3	4	4	3
	2	2	0,00%	0,46%	0,00%	0,46%	1,22%	1	3	2	0	0
			0,00%	0,21%	0,35%	0,23%	0,00%	1	1	1	0	2
	3	2	0,21%	0,00%	0,00%	0,00%	0,00%	0	3	2	0	3
			2,06%	0,00%	0,00%	0,00%	0,84%	1	2	1	2	0

Supplemental table 4: Overview estrous phase of oviducts used. Determined on the basis of the attached oocyte and its corpus luteum (Ireland et al., 1980; Senger, 1997).

Section	Experiment	Replicate	Phase estrous cycle
I	12-, 15- 23-days	1	Not determined
	6-weeks	1	Not determined
	Pooled vs. non-pooled	1	
	Non-pooled animal 1		Diestrus
	Non-pooled animal 2		Early to late metestrus
	Non-pooled animal 3		Diestrus
	Pooled		Pooled animal 1, 2 & 3
II	EDC exposure	1	Diestrus
			Diestrus
			Proestrus
			Diestrus
		2	Proestrus
			Diestrus
			Follicular phase
			Late metestrus
		3	Diestrus
			Follicular phase
			Proestrus
			Follicular phase
III	SOF incubation (replicate 1 & 2)	1	Diestrus
	Embryo co-culture (replicate 1)		Diestrus
			Proestrus
			Diestrus
		2	Proestrus
			Diestrus
			Follicular phase
			Late metestrus

Appendix

Diethylstilbestrol (DES) exposure during *in vitro* embryo culture (IVC)

To assess the effect of DES exposure on early embryonic development, presumed zygotes were exposed during *in vitro* embryo culture (IVC) to DES (10^{-9} M, 10^{-7} M, 10^{-5} M).

Materials and Methods

In vitro embryo production (IVP)

Oocyte collection, *in vitro* maturation (IVM), *in vitro* fertilization (IVF), and *in vitro* embryo culture (IVC) were performed as described in the *in vitro* embryo production (IVP) protocol (materials and methods; methods; IVP; page 16). For IVP solutions see materials and methods; media solutions; IVP; page 9-10.

Diethylstilbestrol (DES) exposure during IVC

Presumed zygotes were exposed from IVC day 1-5 to diethylstilbestrol (DES; #D4628-1G Sigma-Aldrich, St. Louis, MO, United States). SOF was supplemented with DES (10^{-9} M, 10^{-7} M, 10^{-5} M) or 0.01% v/v DMSO (vehicle; D2650-5X Sigma-Aldrich, St. Louis, MO, United States). Plain SOF medium was used as control. At day 5, exposed embryos were transferred to fresh SOF without DES or vehicle and cultured until day 8.

Results: DES exposure during *in vitro* embryo culture does not affect early embryo cleavage and blastocyst rate

Previously, it was reported that there were no statistical significant changes in early embryo cleavage and blastocyst rate after exposure (Asimaki et al., 2022). Experiment was replicated and the cleavage rate at day 5, and blastocyst rate at day 7 and 8 were reported. DES (10^{-9} M, 10^{-7} M, 10^{-5} M) exposure during IVC did not have a statistically significant effect in cleavage rate (80%, 77%, 80%, respectively) compared to control and vehicle-treated (75,6%, 80,9%, respectively) (Supplemental Figure 1A). Additionally, as previously mentioned, day 8 blastocyst yield for this IVP protocol was around 30-40%, control and vehicle-treated monolayers reached 34% day 8 blastocyst rate, whereas DES treated (10^{-9} M, 10^{-7} M, 10^{-5} M) presumed zygotes had day 8 blastocyst rates of 30%, 29%, and 27%, respectively (Supplemental Figure 1B). No statistically significant difference in day 8 blastocyst rates were observed, indicating that DES exposure during IVC does not affect blastocyst rate.

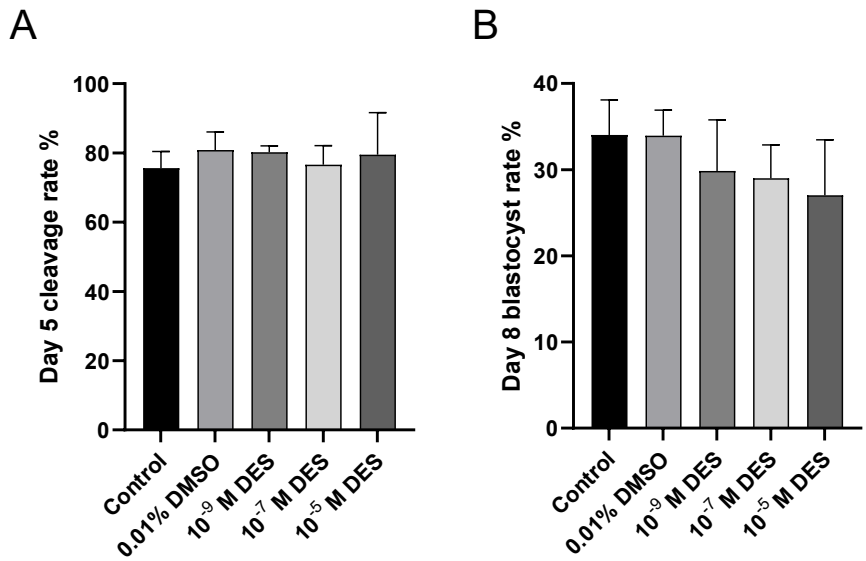

Supplemental Figure 1: Presumed zygotes exposed to DES (10^{-9} M, 10^{-7} M, 10^{-5} M) during IVC day 1-5. (A) Day 5 cleavage rate. (B) Day 8 blastocyst rate. Bars represent mean ± SD of four replicates.